

1 **Reliability Improvement of Wind Turbine Power Generation using Model-based Fault Detection and Fault**
2 **Tolerant Control: a review**

3 Hamed Habibi¹, Ian Howard¹, and Silvio Simani²

4 ¹Faculty of Science and Engineering, School of Civil and Mechanical Engineering, Curtin University, Perth,
5 Australia.

6 ²Department of Engineering, University of Ferrara, Ferrara, Italy.

7 H. Habibi is the corresponding author (e-mail: hamed.habibi@postgrad.curtin.edu.au).

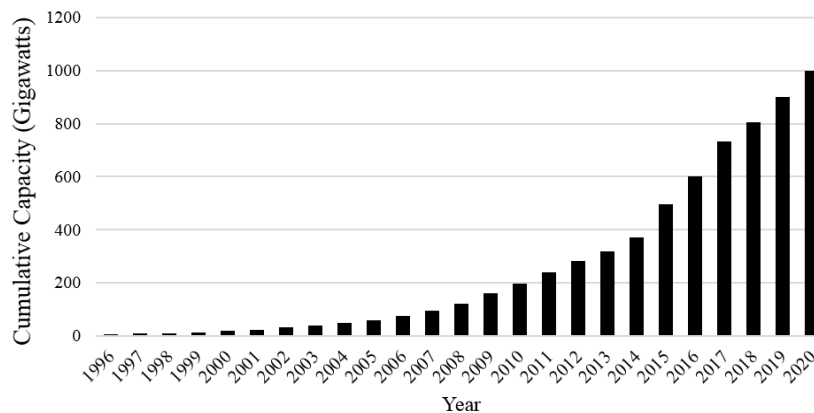
8 **Abstract**

9 Reliability improvement of wind turbine power generation is the key issue that can turn the wind power into one of
10 the main power sources to respond to the world power demands. The likelihood of fault occurrence on wind turbine
11 components is unavoidable, especially for large rotor modern wind turbines, operating in harsh offshore environments.
12 Accordingly, the maintenance need increases due to unanticipated faults, which in turn, leads to higher energy cost
13 and less reliable power generation. In this regard, model-based fault detection and fault tolerant control techniques
14 have been extensively investigated in the last decade, for achieving good performance. In this way, the reliability,
15 availability and safety features of the wind turbine power generation are also enhanced. Thus, in this paper a
16 comprehensive review of the most-recent model-based fault detection and fault tolerant control schemes for wind
17 turbine power generation is presented, focusing on the advantages, capabilities and limitations. Note that the so-called
18 data-driven or signal-based methodologies, which rely on the analysis of the signals directly generated from the
19 monitored system, are not reviewed in this paper. This review is organized in a tutorial manner, to be a suitable
20 reference for further research for the wind turbine's reliability improvement.

21
22 *Keywords: Wind Turbines; Model-based approaches; Reliability and robustness; Fault Detection and Isolation*
23 *(FDI); Fault estimation; Fault Tolerant Control (FTC).*

24
25 **1. Introduction**

26 Ever increasing energy demand is one of the key factors forming the energy research trends. The decrease in
27 exploitable sources, huge environmental pollution, and high price, are some of the most reported problems of the
28 traditional energy resources. As the result of seeking for new resources, the renewable energy resources have been
29 ascertained as an appropriate alternative to traditional fossil fuel energy generation, among which wind energy has
30 demonstrated outstanding characteristics and has attracted the world's attention; therefore, it has been defined as "the
31 world's fastest-growing renewable energy source" with 30% growth annually on average throughout the last two
32 decades [1]. During this time, the planned capacity of wind farms has increased significantly to provide a higher share
33 of the energy. The global wind power installations are illustrated in Figure 1, which also depicts the growth of captured
34 wind power. The wind power extraction of some countries has also been summarized in Table 1, which shows the
35 anticipated growth and demand for wind power. Accordingly, modern wind turbines are designed with a longer blade,
36 to increase the swept area, with higher towers and also to be located in remote offshore places to encounter higher
37 wind speeds, and consequently, to increase the captured power e.g. from 75-kW to 20-MW [2], as illustrated in Table
38 2.



39
40
41
42
43
Fig. 1. Global capacity of wind power plant [1, 3].

44

Table 1. Wind power share of whole power demand for some countries.

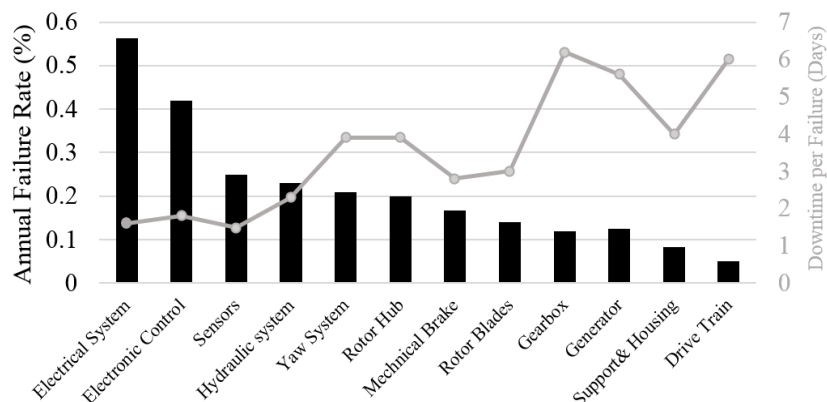
Country	Wind power share of whole demand	Expected year	Reference
United States	30% (300 GW)	2030	[2]
European Union	12-14%	2020	[4, 5]
	25%	2030	
China	15%	2020	[1, 4]
Portugal, Spain, France, Germany, Ireland, Sweden	9% to 21%	2015	[1, 5]
Denmark	50%	2020	[6]

45
46

Table 2. Wind turbine size increase throughout the last three decades [1].

Blade length (m)	Tower height (m)	Nominal power (kW)	Usage year	Location
8.5	30	75	1980-1990	Onshore
15	45	300	1990-1995	Onshore
25	60	750	1995-2000	Onshore
35	70	1500	2000-2005	Onshore
40	95	1800	2005-2010	Onshore
50	100	3000	2010-present	Onshore
62.5	130	5000	2010-present	Offshore
75	160	10000	Future	Onshore
125	220	20000	Future	Offshore

47 The operation of large offshore wind turbines in harsh environments and in the presence of highly varying stochastic
 48 loads, often leads to the occurrence of faults, requiring increased planned maintenance schedules [7, 8]. This presents
 49 the major problem of the lower reliability of wind power generation [9]. Increased maintenance has double negative
 50 effects, i.e. higher maintenance cost and also, less generated power due to increased downtime [10, 11]. Accordingly,
 51 the cost of the generated energy is generally increased and, consequently, the wind turbine generated power may be
 52 less competitive compared to other traditional resources. For example, the maintenance cost of an offshore wind
 53 turbine is estimated to be 20-25% of the total income [12-14] and 10-15% for an onshore farm for 20 years of operating
 54 life [15]. In Figure 2, the wind turbine failure rates and corresponding downtime are illustrated [8]. It is thus beneficial
 55 to keep the maintenance cost as low as possible, decrease downtime and, consequently increase the captured power,
 56 and finally improve reliability, despite the presence of faults [16]. For this aim, Fault Detection and Isolation (FDI)
 57 and Fault Tolerant Control (FTC) are powerful methods. The fault information captured from FDI units can be used
 58 to optimize the maintenance procedures via remote diagnosis [17]. The use of FTC allows the equipment to achieve
 59 the required robustness with respect to the considered faults and, consequently, keeps the wind turbine performance
 60 at the desired level, despite the presence of faults. So, the maintenance need and downtime are decreased, and the
 61 reliability of power generation will be improved. Therefore, the final cost is kept as cheap as possible [18, 19].
 62



63
64
65
66
67
68
69

Fig. 2. Wind turbine component failure rate (black color) and downtime (grey color) [8].

The FDI and FTC designs for wind turbines have been significantly developed over the last decade. Most of the works in this field have been motivated by the competitions conducted by KK-electronic a/c and MathWorks from 2009 to 2015 [17]. Accordingly, the number of studies and consequent publications has been increased considerably. In Figure 3, SCOPUS results have been presented to highlight the rapid growth by considering the published journal papers in

70 the field of wind turbine FDI and FTC, which implies that it currently represents the subject of intensive worldwide
71 research [20]. However, there are only a few available review papers in this field [21-24]. So, it is beneficial to have
72 a well-organized comprehensive overview on the status of recent developments of FDI and FTC techniques for wind
73 turbine power control, to make a framework for future studies, as the motivation of the current paper. Accordingly, in
74 Section 2, the wind turbine model including faults is described. Also, modern wind turbine model representations for
75 FDI purposes are recalled. In Section 3, the different available FDI methods are outlined. Consequently, the FDI
76 methods for each component of the wind turbine are summarized in Section 4. FTC design techniques for wind
77 turbines are sketched in Section 5. Finally, the concluding discussion, future trends on this area and conclusions are
78 given in Sections 6 and 7, respectively.

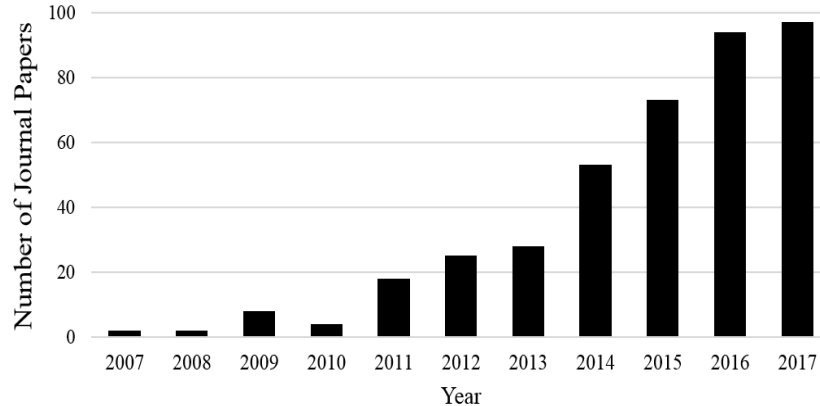


Fig. 3. SCOPUS indexed published journal papers in the field of FDI and FTC wind turbine design.

79
80

2. Wind turbine model representation for fault detection purposes

81 The wind turbine modeling framework specifies appropriate FDI methods. Obviously, the nonlinear model provides
82 the best framework, on which basis it can be used to design the FDI scheme, as it is able to accurately represent the
83 wind turbine behavior [25]. Nevertheless, it leads to more complicated FDI structures. On the other hand, model-based
84 FDI methods have been mostly developed for linear models. Consequently, the linearized wind turbine model has
85 dominated the recent research scope [1, 26-29]. Nevertheless, inconsistency between behaviors of the linearized model
86 and the highly nonlinear wind turbine is significant. So, to have more accurate model representation as well as to take
87 advantage of already-developed FDI methods, two modern wind turbine modelling frameworks have been recently
88 proposed, including linear parameter varying (LPV) and fuzzy Takagi-Sugeno (T-S) prototypes, which are briefly
89 recalled in this section. It should be noted that several high-fidelity wind turbines model packages already exist, e.g.
90 the Fatigue, Aerodynamics, Structures, and Turbulence (FAST) tool developed by NREL [21], and the 4.8MW wind
91 turbine benchmark model developed by KK-electronic A/C and Aalborg University [17]. However, to review the fault
92 sources and effects, the wind turbine model is briefly introduced.

2.1. Nonlinear model and possible faults

94 The wind turbine operation can be seen as an interaction between wind speed and blades. Accordingly, due to the
95 given aerodynamic profile of the blades, aerodynamic torque and thrust are applied to the rotor shaft, i.e. connected
96 directly to the blades, and nacelle, respectively. The wind speed is usually modelled as the sum of a steady state mean
97 value, and stochastic perturbation terms, considering turbulence and gusts. The mean wind speed is estimated by
98 passing a set of measured wind data through a low-pass filter. On the other hand, the stochastic term can be modelled
99 using Von Karman or Kaimal turbulence models [30]. In addition, the wind shear effect, i.e. variation of wind speed
100 depending on height, and periodic tower shadow effect, i.e. wind speed reduction for the blade passing in front of the
101 tower, are two deterministic terms, for which there are accurate mathematical expressions that can be implemented in
102 the wind speed model [26].

103 In variable pitch wind turbine types, the aerodynamic performance of the blades can be changed by adjusting the blade
104 pitch angles. The rotor shaft speed is increased and transferred into the generator shaft using a drivetrain in between.
105 Finally, the electrical power is produced in the generator. In variable speed wind turbine types, the electrical generator
106 torque load can be tuned to control shaft speed. All the mentioned components are located in the nacelle at the top of
107 the tower. The applied aerodynamic thrust leads to a fore-aft oscillation of the tower, which varies the effective wind
108 speed at the blade plane. Also, a yaw mechanism is used to rotate and keep the wind turbine perpendicular to the wind
109 direction, measured with a wind vane, although, at the control system level, due to limited yaw rate, i.e. less than 1°/s,
110 the yaw mechanism is often ignored [22].
111

112 The blade aerodynamic characteristics can be characterized with $C_p(\beta, \lambda)$, $C_q(\beta, \lambda)$ and $C_t(\beta, \lambda)$, which are power
 113 coefficient, aerodynamic coefficient and thrust coefficient, respectively. These coefficients are functions of β , i.e.
 114 blade pitch angle and λ , i.e. tip speed ratio, defined as $\lambda = R\omega_r/V_r$, where R is blade length, ω_r is blade rotor angular
 115 speed and V_r is the effective wind speed at the rotor plane. These coefficients are often available as numerical lookup
 116 tables or empirical equations for a given blade profile. The aerodynamic torque T_a , power P_a and thrust F_t , are as,

$$T_a = \frac{1}{2}\rho ARV_r^2 C_q(\beta, \lambda), P_a = \frac{1}{2}\rho AV_r^3 C_p(\beta, \lambda), F_t = \frac{1}{2}\rho AV_r^2 C_t(\beta, \lambda), \quad (1)$$

117 respectively, where, ρ is air density and A is blade swept area as, $A = \pi R^2$. Also, the power coefficient can be
 118 represented as $C_p(\beta, \lambda) = \lambda C_q(\beta, \lambda)$. Considering fore-aft oscillation of the nacelle, due to F_t , the effective wind speed
 119 can be represented as a relative velocity as, $V_r = V_w - V_n$, where V_w is the free wind speed before encountering the
 120 blades and V_n is the projected nacelle velocity in the wind direction. Considering modern wind turbines with three
 121 independent pitch actuator mechanisms, the resultant aerodynamic torque can be written as,

$$T_a = \frac{1}{6} \sum_{i=1}^3 \rho ARV_r^2 C_q(\beta_i, \lambda), \quad (2)$$

122 where, β_i is the pitch angle of the i^{th} blade.

123 Long term operation of the wind turbine may lead to debris build-up on the blades, due to dirt or ice, and erosion. This
 124 changes the blades aerodynamic characteristics, as deviation of C_p , C_q and C_t mappings from normal ones [29]. The
 125 debris build-up effect is modelled as,

$$\tilde{C}_p = C_p + \Delta C_p, \tilde{C}_q = C_q + \Delta C_q, \tilde{C}_t = C_t + \Delta C_t. \quad (3)$$

126 In this paper, $\tilde{\chi}$ and $\Delta\chi$ are the new abnormal value and deviation from the normal parameter χ , respectively.

127 The rotor speed ω_r is increased and transferred into the generator shaft, rotating at ω_g , via the drivetrain, which can
 128 be modelled as a two degree of freedom rotational system. Inertia of rotor and generator shafts are J_r and J_g ,
 129 respectively. Also, the drivetrain speed ratio is N_g and includes torsion stiffness K_{dt} and torsion damping, B_{dt} . This
 130 elastic gear meshing results in a torsional angle of twist of the main shaft θ_Δ , which is defined as $\theta_\Delta = \theta_r - \theta_g/N_g$,
 131 where, θ_r and θ_g are rotation angle of rotor and generator shafts, respectively. Also, viscous frictions for rotor and
 132 generator shaft bearings are considered whose coefficients are B_r and B_g , respectively. The drivetrain efficiency in
 133 transferring speed is η_{dt} [26, 31]. The drivetrain model is then written as,

$$\begin{aligned} \dot{\omega}_r(t) &= -\left(\frac{B_r+B_{dt}}{J_r}\right)\omega_r(t) + \frac{B_{dt}}{J_r N_g}\omega_g(t) - \frac{K_{dt}}{J_r}\theta_\Delta(t) + \frac{1}{J_r}T_a(t), \\ \dot{\omega}_g(t) &= \frac{\eta_{dt}B_{dt}}{N_g J_g}\omega_r(t) - \left(\frac{B_g}{J_g} + \frac{\eta_{dt}B_{dt}}{J_g N_g^2}\right)\omega_g(t) + \frac{\eta_{dt}K_{dt}}{N_g J_g}\theta_\Delta(t) - \frac{1}{J_g}T_g(t), \\ \dot{\theta}_\Delta(t) &= \omega_r(t) - \frac{1}{N_g}\omega_g(t). \end{aligned} \quad (4)$$

134 where, T_g is generator shaft torque. The wear or tear of drivetrain gears can be considered to be possible faults in this
 135 mechanism, which changes the drivetrain stiffness and damping, considered as, $\tilde{K}_{dt} = K_{dt} + \Delta K_{dt}$ and $\tilde{B}_{dt} = B_{dt} +$
 136 ΔB_{dt} [17, 18]. This fault happens very slowly with time, but it leads to total drivetrain breakdown which results in
 137 long and costly downtime [17].

138 The pitch actuator is modeled as an underdamped hydraulic mechanism, which is more reliable with little backlash
 139 and larger stiffness than the electrical pitch actuator motor. The hydraulic pitch actuator is thus described as a second
 140 order dynamic system as,

$$\ddot{\beta} = -\omega_n^2\beta - 2\omega_n\xi\dot{\beta} + \omega_n^2\beta_{ref}, \quad (5)$$

141 where, ω_n and ξ are the natural frequency and damping ratio of the pitch actuator, respectively. Also, β_{ref} is the
 142 reference pitch angle, commanded by the pitch controller and to be followed by blade pitch angle. The operational
 143 ranges of the pitch actuator are considered as $\hat{\beta}_{min} \leq \hat{\beta} \leq \hat{\beta}_{max}$, $\beta_{min} \leq \beta \leq \beta_{max}$. In this paper, χ_{max} and χ_{min}
 144 stand for maximum and minimum allowable values of the variable χ , respectively. The pitch actuator may suffer from
 145 dynamic change which leads to slower response and, consequently, poor pitch angle regulation [32]. Three of the most
 146 reported dynamic changes are hydraulic pump wear, pressure drop due to hydraulic leakage and more compressible
 147 oil due to high air content in the hydraulic oil. These dynamic changes deviate the natural frequency and damping
 148 ratio from normal values [24]. It should be noted that hydraulic leakage is considered as an abrupt fault while oil air
 149 content increases slowly. The numerical values of a given pitch actuator dynamic changes presented for a wind turbine
 150 benchmark model, [33], are summarized in Table 3, in which PW , HL and HAC stand for pump wear, hydraulic
 151 leakage and high air content situations, respectively. $\omega_{n,X}$ and ξ_X are natural frequency and damping ratio,
 152 respectively, in the situation X . α_{f_1} and α_{f_2} are fault indicators.

153
 154

155
156
157

Table 3. Numerical values of a given pitch actuator dynamic changes [33].

	Natural Frequency(rad/s)	Damping Ratio	Fault Indicator
Normal	$\omega_{n,N} = 11.11$	$\xi_N = 0.6$	$\alpha_{f_1} = \alpha_{f_2} = 0$
Pump Wear	$\omega_{n,PW} = 7.27$	$\xi_{PW} = 0.75$	$\alpha_{f_1} = 0.6316, \alpha_{f_2} = 0.29688$
Hydraulic Leak	$\omega_{n,HL} = 3.42$	$\xi_{HL} = 0.9$	$\alpha_{f_1} = 1, \alpha_{f_2} = 0.87853$
High Air Content	$\omega_{n,HAC} = 5.73$	$\xi_{HAC} = 0.45$	$\alpha_{f_1} = 0.81083, \alpha_{f_2} = 1$

158
159
160
161
162

The pitch actuator long-term operation may lead to an actuator fault, modelled as an additive bias β_{bias} . Indeed, this fault deviates the desired pitch actuator β to $\beta + \beta_{bias}$. Also, the dynamic changes can be considered as a convex function of normal natural frequency and normal damping ratio. So, the pitch actuator (5) including the dynamic change and bias can be rewritten as,

$$\ddot{\beta} = -\omega_{n,N}^2(\beta + \beta_{bias}) - 2\omega_{n,N}\xi_N\dot{\beta} + \omega_{n,N}^2\beta_{ref} + \Delta\tilde{f}_{PAD}, \quad (6)$$

163 where, $\Delta\tilde{f}_{PAD} = -\alpha_{f_1}\Delta(\tilde{\omega}_n^2)\beta - 2\alpha_{f_2}\Delta(\tilde{\omega}_n\xi)\dot{\beta} + \alpha_{f_1}\Delta(\tilde{\omega}_n^2)\beta_{ref}$, $\Delta(\tilde{\omega}_n^2) = \omega_{n,HL}^2 - \omega_{n,N}^2$ and $\Delta(\tilde{\omega}_n\xi) =$
 164 $\omega_{n,HAC}\xi_{HAC} - \omega_{n,N}\xi_N$.

165 Remark 1: The hydraulic pitch actuator has fast response time, large control effort (torque), and convenient
 166 centralization [34]. The electrical servo motor is another type of pitch actuator, to avoid the frequent hydraulic pitch
 167 actuator oil leakage and maintenance. Also, this type has more efficient and quicker response time than the hydraulic
 168 one [35]. However, this type of pitch actuator may suffer from overheated motor, cooling fan errors, brake damage,
 169 jams in the bearing and short circuits of the winding. Also, the battery system failure is considerable when the charger
 170 is not available [36]. In this case, the battery cannot provide enough power to pitch the blades. The electrical pitch
 171 actuator can be represented as a first order system as $\dot{\beta}(t) = -a_\beta\beta(t) + a_\beta\beta_{ref}(t)$, where $a_\beta = 1/\tau_\beta$ and τ_β is the
 172 pitch actuator time constant [1, 37]. For example, τ_β is selected as 50 ms in [38], which is obviously negligible
 173 compared to the slow mechanical response of wind turbines. The mentioned electrical pitch actuator failures can be
 174 augmented in this equation as dynamic change, i.e. change in time constant $\Delta\tau_\beta$ and pitch angle offset f_β , as, $\dot{\beta}(t) =$
 175 $-a_\beta(\beta(t) + f_\beta) + a_\beta\beta_{ref}(t) + \Delta\tilde{f}_{PAD}(t)$, where, $\Delta\tilde{f}_{PAD}(t) = -\Delta a_\beta(\beta(t) + f_\beta) + \Delta a_\beta\beta_{ref}(t)$ and $\Delta a_\beta = -\Delta\tau_\beta/$
 176 $(\tau_\beta^2 + \tau_\beta \cdot \Delta\tau_\beta)$. It should be pointed out that both the hydraulic and electrical pitch actuators can be represented as a
 177 first or second order system, though in practice, both are often represented as a second order system. Consequently,
 178 the electromechanical pitch actuator can be considered as fourth order system; two modes for the electric part, and
 179 two modes for the mechanical one [39]. Moreover, as the blade inertia is contributing in the mechanical mode, for the
 180 wind turbines with large blades, the dynamics of the mechanical part are dominant. So, the system can be approximated
 181 as a second order model. For this second order model, the natural frequency and damping ratio are $\omega_n =$
 182 11.11 (rad/s) and $\xi = 0.6$, respectively. However, it is stated that for electromechanical pitch systems, which are
 183 more widespread in use, a first-order delay model may be sufficient [37, 39].

184 The generator converts shaft kinetic energy into electrical energy. Doubly-Fed Induction Generators (DFIG) are one
 185 of the most commonly used generator configurations [30]. In modern wind turbines, the frequency of produced
 186 electricity is adjusted by current control via a converter to enable variable speed operation [33]. Indeed, the converter
 187 acts as an interface between the generator and the grid. The converter is modelled as a first-order system with time
 188 delay τ_g to track the requested generator torque load $T_{g,ref}$ as,

$$\dot{T}_g = -a_g T_g + a_g T_{g,ref}, \quad (7)$$

189 where, $a_g = 1/\tau_g$ and T_g refers to generator shaft torque. The wind turbine internal electronic controller is much faster
 190 than the slow mechanical dynamic behavior. Accordingly, the produced electrical power in the generator P_g is
 191 approximated as a static relation as $P_g = \eta_g \omega_g T_g$ where η_g is the generator efficiency. Achievable generator torque
 192 and its variation, are considered to be limited as, $\dot{T}_{g,min} \leq \dot{T}_g \leq \dot{T}_{g,max}, T_{g,min} \leq T_g \leq T_{g,max}$ [33]. Internal electric
 193 faults in the converter, manufacturing defects and initialization of the converter controller, lead to either generator
 194 torque offset f_{T_g} or increased converter delay $\Delta\tau_g$ [20, 21, 40]. Although, the converter controller would typically be
 195 able to detect and accommodate $\Delta\tau_g$. So, the converter model (7) is rewritten as,

$$\dot{T}_g = -a_g(T_g + f_{T_g}) + a_g T_{g,ref} + \Delta\tilde{f}_{GC}, \quad (8)$$

196 where, $\Delta\tilde{f}_{GC} = -\Delta a_g(T_g + f_{T_g}) + \Delta a_g T_{g,ref}$ and $\Delta a_g = -\Delta\tau_g/(\tau_g^2 + \tau_g \cdot \Delta\tau_g)$.

197 The main available wind turbine measurements are rotor speed, generator speed, pitch angle and generator torque. All
 198 measurements are assumed to contain unavoidable random noise [21]. Different sensor technologies are typically

199 adopted on wind turbines, e.g. strain gauge, piezoelectric, encoder, optical and laser sensors [10]. As most of the
 200 control schemes are designed based on the feedback of sensor measurements, sensor noise and faults lead to
 201 performance degradation or even instability. Lightning, moisture, salt spray and corrosion, may cause sensor faults.
 202 Also, blade misalignment at the installation step or during operation, leads to pitch sensor faults. Also, if the encoder
 203 is used for shaft speed estimation, loss of metal pieces on the shaft leads to inaccurately measured speed. Moreover,
 204 malfunctions of the electrical components of the encoders represent another reported source of faults [21]. On the
 205 other hand gearbox resonance frequency content on the generator speed sensor may deviate the sensor output from
 206 accurate readings [41]. In the modern wind turbines, to fulfill the physical redundancy concept, i.e. the most reliable
 207 configuration for FDI, the pitch angle, rotor speed and generator speed are measured with two separate identical
 208 sensors [42]. The sensor faults can be modelled as different fault types as, additive constant bias, gained multiplicative
 209 measurement, fixed and no sensor outputs. The measurement of variable X including sensor fault and noise content is
 210 given as, $X_s = X + v_x + X_{bias}$, where X_s is the measured signal, v_x is random noise content and X_{bias} is the additive
 211 time variable bias, to take other sensor fault types into consideration. This fulfils the nonlinear description of wind
 212 turbine models associated with different fault sources. The considered faults in the wind turbine model are summarized
 213 in Table 4, in which the fault characteristics are stated.

214 **2.2. Linearized model associated with faults**

215 The aerodynamic behavior of wind turbines is a highly nonlinear function of blade pitch angle, wind speed and rotor
 216 speed, as (1). So, the nonlinear wind turbine model, i.e. (2), (4), (6) and (8), is usually linearized around different
 217 operation points. Considering the desired operation trajectory as $\overline{OP} = (\overline{V}_r, \overline{\beta}, \overline{\omega}_r)$, the linear aerodynamic behavior is
 218 represented via the linearization of (2) as,

$$T_a = T_{a,V_r} \tilde{V}_r + \frac{1}{3} \sum_{i=1}^3 T_{a,\beta_i} \tilde{\beta}_i + T_{a,\omega_r} \tilde{\omega}_r, \quad (9)$$

219 where, $T_{a,V_r} = (\partial T_a / \partial V_r)|_{\overline{OP}}$, $T_{a,\beta_i} = (\partial T_a / \partial \beta_i)|_{\overline{OP}}$, $T_{a,\omega_r} = (\partial T_a / \partial \omega_r)|_{\overline{OP}}$, $\tilde{V}_r = V_r - \overline{V}_r$, $\tilde{\beta}_i = \beta_i - \overline{\beta}$ and $\tilde{\omega}_r =$
 220 $\omega_r - \overline{\omega}_r$. Now, the linearized wind turbine model including all considered faults, is summarized as,

$$\dot{\mathbf{x}} = \mathbf{A}\mathbf{x} + \mathbf{B}\mathbf{u} + \mathbf{F}_a \mathbf{f}_a + \mathbf{R}V_r, \quad (10)$$

221 where, $\mathbf{x} = [\omega_r, \omega_g, \theta_\Delta, T_g, \beta_1, \dot{\beta}_1, \beta_2, \dot{\beta}_2, \beta_3, \dot{\beta}_3]^T$, $\mathbf{u} = [T_{g,ref}, \beta_{ref,1}, \beta_{ref,2}, \beta_{ref,3}]^T$, $\mathbf{f}_a =$
 222 $[\Delta f_{1,DT}, \Delta f_{2,DT}, \Delta f_{GC}, \Delta f_{PAD,1}, \Delta f_{PAD,2}, \Delta f_{PAD,3}]^T$, $\mathbf{R} = [T_{a,V_r}/J_r, 0, 0, 0, 0, 0, 0, 0, 0]^T$, where, $\Delta f_{1,DT} = -\Delta B_{dt} \omega_r / J_r +$
 223 $\Delta B_{dt} \omega_g / J_r N_g - \Delta K_{dt} \theta_\Delta / J_r$, $\Delta f_{2,DT} = \eta_{dt} \Delta B_{dt} \omega_r / N_g J_g - \eta_{dt} \Delta B_{dt} \omega_g / J_g N_g^2 + \eta_{dt} \Delta K_{dt} \theta_\Delta / N_g J_g$, $\Delta f_{GC} = -a_g f_{T_g} +$
 224 $\Delta \tilde{f}_{GC}$, $\Delta f_{PAD,i} = -\omega_{n,N}^2 \beta_{bias,i} + \Delta \tilde{f}_{PAD,i}$, $\Delta \tilde{f}_{PAD,i} = -\alpha_{f_1} \Delta(\tilde{\omega}_n^2) \beta_i - 2\alpha_{f_2} \Delta(\tilde{\omega}_n \tilde{\xi}) \dot{\beta}_i + \alpha_{f_1} \Delta(\tilde{\omega}_n^2) \beta_{ref,i}$. $\beta_{bias,i}$ and
 225 $\beta_{ref,i}$ are pitch actuator bias and reference pitch angle of i^{th} blade, respectively.

226 Table 4. The wind turbines fault characteristics.

Components	Symptom	Category	Consequence	Severity	Deviation Time	Symbol	Fault model
Pitch sensor	Biased, gained, fixed and no measurement output	Sensor fault	Poor power optimization in low wind speed and power regulation in high wind speed.	Low	Medium	$\beta_{i,s,j,bias}$	Time variable additive bias
Rotor sensor						$\omega_{r,s,j,bias}$	
Generator sensor						$\omega_{g,s,j,bias}$	
Generator/ Converter	Offset generator torque bias	Actuator fault	Non-optimum power production.	Medium	Fast	f_{T_g}	Additive constant offset
Pitch actuator	Pitch angle bias		Poor power regulation, uneven aerodynamic torque and excited structural modes.			$\beta_{bias,i}$	
Generator/ Converter	Increased time delay	System fault	Slow generator torque control and non-optimal power production.	High	Fast	$\Delta \tau_g$	Added time delay
Pitch actuator	Pump Wear		Slow pitch angle adjustment and consequently poor power regulation.	High	Medium	$\Delta \tilde{f}_{PAD}$	Change in natural frequency and damping ratio
Pitch actuator	High air content in oil			Medium	Slow		
Pitch actuator	Hydraulic leakage			High	Medium		

Drivetrain	Wear and tear		Increased vibrations of drivetrain.	Medium	Very slow	ΔK_{dt} and ΔB_{dt}	Change in stiffness and damping
Blade aerodynamics	Debris build up		Out of designed aerodynamic relation (Non-optimal power production, poor power regulation).	Medium	Very slow	ΔC_p and ΔC_q	Aerodynamic coefficients change

227 Also, $A = \begin{bmatrix} A_{DT} & A_{GI} & A_{AE} \\ \mathbf{0}_{1 \times 3} & A_{GS} & \mathbf{0}_{1 \times 6} \\ \mathbf{0}_{6 \times 3} & \mathbf{0}_{6 \times 1} & A_{PS} \end{bmatrix}$, $A_{DT} = \begin{bmatrix} A_{DT11} & A_{DT12} & A_{DT13} \\ A_{DT21} & A_{DT22} & A_{DT23} \\ 1 & A_{DT32} & 0 \end{bmatrix}$, $A_{GI} = [0 \quad -1/J_g \quad 0]^T$, $A_{AE} =$
 228 $\begin{bmatrix} T_{a,\beta 1}/3J_r & 0 & T_{a,\beta 2}/3J_r & 0 & T_{a,\beta 3}/3J_r & 0 \\ \mathbf{0}_{2 \times 6} \end{bmatrix}$, $A_{GS} = -a_g$, $A_{DT11} = -(B_r + B_{dt})/J_r + T_{a,\omega_r}/J_r$, $A_{DT12} = B_{dt}/$
 229 $J_r N_g$, $A_{DT13} = -K_{dt}/J_r$, $A_{DT21} = \eta_{dt} B_{dt}/N_g J_g$, $A_{DT22} = -B_g/J_g - \eta_{dt} B_{dt}/J_g N_g^2$, $A_{DT23} = \eta_{dt} K_{dt}/N_g J_g$, $A_{DT32} =$
 230 $-1/N_g$, $A_{PS} = \begin{bmatrix} A_{PS1} & \mathbf{0}_{2 \times 2} & \mathbf{0}_{2 \times 2} \\ \mathbf{0}_{2 \times 2} & A_{PS2} & \mathbf{0}_{2 \times 2} \\ \mathbf{0}_{2 \times 2} & \mathbf{0}_{2 \times 2} & A_{PS3} \end{bmatrix}$, $A_{PS1} = A_{PS2} = A_{PS3} = \begin{bmatrix} 0 & 1 \\ -\omega_{n,N}^2 & -2\xi_N \omega_{n,N} \end{bmatrix}$, $B =$
 231 $\begin{bmatrix} \mathbf{0}_{3 \times 1} & \mathbf{0}_{5 \times 1} & \mathbf{0}_{7 \times 1} & \mathbf{0}_{7 \times 1} \\ a_g & \omega_{n,N}^2 & \omega_{n,N}^2 & \mathbf{0}_{2 \times 1} \\ \mathbf{0}_{6 \times 1} & \mathbf{0}_{4 \times 1} & \mathbf{0}_{2 \times 1} & \omega_{n,N}^2 \end{bmatrix}$, $F_a = \begin{bmatrix} 1 & \mathbf{0}_{1 \times 2} & \mathbf{0}_{5 \times 2} & \mathbf{0}_{2 \times 1} \\ \mathbf{0}_{7 \times 1} & F_{a1} & F_{a1} & \mathbf{0}_{7 \times 1} \\ \mathbf{0}_{2 \times 1} & \mathbf{0}_{6 \times 2} & \mathbf{0}_{2 \times 2} & 1 \end{bmatrix}$ and $F_{a1} = \begin{bmatrix} 1 & 0 & 0 \\ 0 & 0 & 1 \end{bmatrix}^T$. The measurement model of
 232 the wind turbine including possible sensor faults and noise contents is written as,

$$233 \quad \mathbf{y} = \mathbf{C}\mathbf{x} + \mathbf{F}_s \mathbf{f}_s + \mathbf{D}, \quad (11)$$

233 where, $\mathbf{y} = [\omega_{r,s,1}, \omega_{r,s,2}, \omega_{g,s,1}, \omega_{g,s,2}, T_g, \beta_{1,s,1}, \beta_{1,s,2}, \beta_{2,s,1}, \beta_{2,s,2}, \beta_{3,s,1}, \beta_{3,s,2}]^T$, $\mathbf{f}_s =$
 234 $[\omega_{r,s,1,bias}, \omega_{r,s,2,bias}, \omega_{g,s,1,bias}, \omega_{g,s,2,bias}, T_{g,bias}, \beta_{1,s,1,bias}, \beta_{1,s,2,bias}, \beta_{2,s,1,bias}, \beta_{2,s,2,bias}, \beta_{3,s,1,bias}, \beta_{3,s,2,bias}]^T$,
 235 $\mathbf{F}_s = \mathbf{I}_{11 \times 11}$, $\mathbf{D} = [v_{\omega_{r,1}}, v_{\omega_{r,2}}, v_{\omega_{g,1}}, v_{\omega_{g,2}}, v_{T_g}, v_{\beta_{1,1}}, v_{\beta_{1,2}}, v_{\beta_{2,1}}, v_{\beta_{2,2}}, v_{\beta_{3,1}}, v_{\beta_{3,2}}]^T$, where, $\omega_{r,s,j}$, $\omega_{g,s,j}$ are the j^{th}
 236 measurement of rotor and generator speeds, respectively, and $\beta_{i,s,j}$ is the j^{th} measurement of the i^{th} pitch angle.
 237 $\omega_{r,s,j,bias}$ and $\omega_{g,s,j,bias}$ are time variable sensor biases of the j^{th} measurement of rotor and generator speeds,
 238 respectively. $T_{g,bias}$ is the generator torque sensor time variable bias. $\beta_{i,s,j,bias}$ is the time variable pitch bias of the
 239 j^{th} measurement of the i^{th} pitch angle. $v_{\omega_{r,j}}$ and $v_{\omega_{g,j}}$ refer to the noise content of the j^{th} measurement of the rotor
 240 and generator speeds, respectively. v_{T_g} is the noise content of the generator torque sensor. $v_{\beta_{i,j}}$ is the noise content of

241 the j^{th} sensor of the i^{th} pitch angle. Also, $\mathbf{C} = \begin{bmatrix} C_1 & \mathbf{0}_{1 \times 2} & \mathbf{0}_{3 \times 1} & \mathbf{0}_{4 \times 2} & \mathbf{0}_{6 \times 2} & \mathbf{0}_{8 \times 2} \\ \mathbf{0}_{1 \times 2} & C_1 & 1 & C_1 & C_1 & C_1 \\ \mathbf{0}_{8 \times 2} & \mathbf{0}_{8 \times 2} & \mathbf{0}_{6 \times 1} & \mathbf{0}_{5 \times 2} & \mathbf{0}_{3 \times 2} & \mathbf{0}_{1 \times 2} \end{bmatrix}^T$, where, $C_1 = [1 \quad 1]$. It
 242 is obvious that the redundancy concept is achieved for rotor speed, generator speed and pitch angle sensors with two
 243 identical sensors.

244 **2.3. Linear parameter varying modelling**

245 The LPV wind turbine modeling framework has emerged in the last decade [43], in which, the wind turbine model is
 246 linearized around several operational points. Accordingly, a set of linearized models is adopted and, according to the
 247 estimated operational point, the proper model is chosen. Indeed, in (2), as wind speed varies, T_a is also variable, which
 248 leads to variation of the matrix A in (10). So, for different wind speeds, different linearized models are obtained.
 249 Consequently, having all possible linearized models as the feasible dynamic descriptor set, leads to the LPV wind
 250 turbine model representation. This provides proper design freedom to achieve robust FDI performance [33, 44].
 251 Considering (10) and for the operation point $OP(k) = (V_r(k), \beta(k), \omega_r(k))$, the overall LPV wind turbine model is
 252 stated as,

$$253 \quad \dot{\mathbf{x}} = A(\theta)\mathbf{x} + \mathbf{B}\mathbf{u} + \mathbf{F}_a \mathbf{f}_a + \mathbf{R}(\theta)V_r, \quad (12)$$

253 where, $A(\theta) = \begin{bmatrix} A_{DT}(\theta) & A_{GI} & A_{AE}(\theta) \\ \mathbf{0}_{1 \times 3} & A_{GS} & \mathbf{0}_{1 \times 6} \\ \mathbf{0}_{6 \times 3} & \mathbf{0}_{6 \times 1} & A_{PS} \end{bmatrix}$, $A_{DT}(\theta) = \begin{bmatrix} A_{DT11}(\theta) & A_{DT12} & A_{DT13} \\ A_{DT21} & A_{DT22} & A_{DT23} \\ 1 & A_{DT32} & 0 \end{bmatrix}$, $A_{DT11}(\theta) = -(B_r + B_{dt})/J_r +$
 254 $(T_{a,\omega_r}/J_r)|_{\theta}$, $A_{AE}(\theta) = \begin{bmatrix} T_{a,\beta 1}/3J_r|_{\theta} & 0 & T_{a,\beta 2}/3J_r|_{\theta} & 0 & T_{a,\beta 3}/3J_r|_{\theta} & 0 \\ \mathbf{0}_{2 \times 6} \end{bmatrix}$ and $\mathbf{R}(\theta) = [T_{a,V_r}/$
 255 $J_r|_{\theta}, 0, 0, 0, 0, 0, 0, 0, 0, 0, 0]^T$. θ is the set of all possible operating points such that $\theta \in \Theta_k$ and $\Theta_k = \{OP(k) \in$
 256 $\mathbb{R}^3 | OP_{min} \leq \|OP(k)\| \leq OP_{max}\}$, where $\|\chi\|$ represents a properly-selected norm operator on variable χ . Indeed, it

257 is assumed that the operational points are bounded. The model (12) includes k linearized models. It should be noted
 258 that the measurement equation is the same as (11). In (12), $\hat{\theta}$, i.e. the estimation of operating point θ , is needed to
 259 accurately implement the LPV representation of the wind turbine.

260 2.4. Fuzzy Takagi–Sugeno modelling

261 In this approach, using multiple linearized models, fuzzy *if-then* rules are defined based on the expert’s knowledge
 262 which combine all the linear models utilizing the T-S prototype [45–49]. The wind turbine measurements can be used
 263 to estimate fuzzy T-S prototype parameters [50]. The fuzzy variable vector \mathbf{Z} is defined as, $\mathbf{Z}(t) = [\omega_r, \beta, V_r]$. Assume
 264 q fuzzy rules are defined as, if ω_r is M_{1i} and β is M_{2i} and V_r is M_{3i} , then $\dot{\mathbf{x}} = A_i \mathbf{x} + \mathbf{B} \mathbf{u} + F_a \mathbf{f}_a + \mathbf{R}_i$, for $i = 1, \dots, q$.
 265 M_{li} are fuzzy membership functions for $l = 1, 2, 3$. Also, A_i and \mathbf{R}_i are the expert-defined dynamic system matrix and
 266 disturbance vector, respectively. The complete fuzzy T-S wind turbine model is represented as,

$$\dot{\mathbf{x}} = \sum_{i=1}^q \mu_i(\mathbf{Z}(t)) (A_i \mathbf{x} + \mathbf{B} \mathbf{u} + F_a \mathbf{f}_a + \mathbf{R}_i V_r), \quad (13)$$

267 where, $\mu_i(\mathbf{Z}(t)) = h_i(\mathbf{Z}(t)) / \sum_{i=1}^q h_i(\mathbf{Z}(t))$ and $h_i(\mathbf{Z}(t)) = \prod_{l=1}^3 M_{li}(\mathbf{Z}(t))$. The measurement equation is the same
 268 as (11). In (13), the expert’s knowledge plays a vital role to properly define the fuzzy rules, dynamic matrix A_i and
 269 disturbance vector \mathbf{R}_i . Otherwise, the designed model is not able to represent the wind turbine dynamic response.

270 3. Fault detection methods applied to wind turbines

271 FDI can be utilized as a fully/partly automatic scheme to detect and locate the possibly occurring faults on the wind
 272 turbine to optimize the required maintenance procedures, reduce downtime, and to avoid catastrophic failure. The
 273 modern maintenance strategies aim to reduce human intervention by implementing hardware or software redundancy
 274 on the wind turbines to automatically detect the faults based on the collected and analyzed data and, consequently, to
 275 reduce/remove the fault effects.

276 Hardware redundancy involves equipping the components such as sensors and actuators, with physically identical
 277 counterparts to generate so-called residual signatures which contain the possible fault information. This approach
 278 increases the weight, occupied space, data acquisition complexity and, consequently, final design cost. These issues
 279 are very problematic for offshore wind turbines. In contrast, software redundancy or computer-based FDI techniques
 280 have been developed on wind turbines during the last decade to overcome the aforementioned problems [51], in which
 281 the mathematical model of the wind turbine is used to generate the redundant signals and, accordingly, residuals.

282 It should be pointed out that there exist other faults in the wind turbine structure which are not mentioned in Table 4.
 283 For instance, degradation of drivetrain lubrication oil which leads to high bearing temperature and, consequently,
 284 lubrication oil ageing. Also, due to wind gusts and consequent temporary misalignment of rotor and generator shafts,
 285 the bearings and gears are damaged [52]. Blade cracks, bearing wear and spalls, gear teeth cracks, generator winding
 286 damage and overheating, are some other reported wind turbine faults. Condition monitoring methods based on
 287 Supervisory Control and Data Acquisition (SCADA), structural health monitoring techniques, frequency spectrum
 288 analysis and vibration signal processing are the main approaches to detect these aforementioned faults [53–55]. Fourier
 289 transformation analysis [56], wavelet methods [57], manifold learning [58], support vector machines [47, 59, 60],
 290 vibration-based condition analysis [57], thermography, strain measurements and acoustic monitoring [18, 61] are some
 291 examples of condition monitoring. All these methods can be categorized as signal-based (or data-driven) fault
 292 detection and there are rich reviews on applying these methods on wind turbines [18, 52, 54, 62–66], so these methods
 293 are not repeated here. On the other hand, yaw actuator faults, whether actuator malfunction or a stuck brake is not
 294 considered, because the yaw mechanism is mostly considered as an on/off actuator and, accordingly, inactive [40].

295 The most challenging issue, which should be considered in wind turbine FDI schemes, is that the wind speed is poorly
 296 measured by the anemometer due to spatial/temporal effective wind speed distribution over the blade plane,
 297 turbulence, wind shear and tower shadow effects. So, wind speed is considered as an unknown disturbance as well as
 298 consequent aerodynamic torque. Also, FDI schemes should be robust against the considerable noise content of sensor
 299 measurements [67]. In this section, the wind turbine model-based FDI techniques are reviewed. Also, to have a
 300 comprehensive and fruitful review, the FDI methods are categorized systematically, which are summarized in Figure
 301 4.

302 3.1. Residual-based approach

303 The residual-based design represents one of the most common wind turbine FDI techniques to detect different faults.
 304 This approach relies on the residual signal obtained by comparing the wind turbine output and the corresponding
 305 duplicated one, which carries any probable fault information. In model-based residual generation, despite physical
 306 redundancy techniques, the redundant measurements can be obtained via the wind turbine mathematical models (see
 307 Section 2), or via design of an appropriate observer. Finally, by adopting an appropriate residual signal evaluation, the
 308 fault is detected [68]. The most commonly adopted residual-based FDI techniques for wind turbines are the parity
 309 relation method [69] and observer design [70]. Generally, the residual vector is defined as,

$$\mathbf{d} = \mathbf{y}_m - \mathbf{y}_w, \quad (14)$$

310 where, \mathbf{y}_m is the wind turbine output vector and \mathbf{y}_w is the wind turbine duplicated output vector. In (14), for the sake
 311 of consideration, the vector \mathbf{d} contains all sensors and duplicated output information. Although, it can be constructed
 312 for one sensor to reduce complexity of the residual evaluation.

313 The widely-exploited residual evaluation methods are simple geometric logic (e.g. threshold check), statistical scheme
 314 (e.g. statistical feature extraction), and Bayesian approaches. In the first approach, an adaptive or fixed threshold σ_{th}
 315 is selected, from which if \mathbf{d} violates, the faults are detected [71]. Indeed, if $\|\mathbf{d}\| > \sigma_{th}$, then the fault is detected,
 316 otherwise no fault has occurred. It should be noted that the presence of measurement errors, disturbance and
 317 uncertainty, may lead to false fault detection. Indeed, these effects may cause \mathbf{d} to be greater than σ_{th} , when no fault
 318 has occurred [72]. Also, by selecting too large a σ_{th} , to avoid false detection, some faults with small effect on \mathbf{d} are
 319 not detected, which may yet cause major operational deficiency, leading to the missed detection problem. So, statistical
 320 analysis of the residual signal can be considered to provide more accurate residual evaluation. Generalized likelihood
 321 ratio test, cumulative variance index and the use of up and down counters, are some statistical analysis methods. These
 322 methods are available e.g. in [51, 73]. The Bayesian approach for residual evaluation will be outlined in Section 3-5.

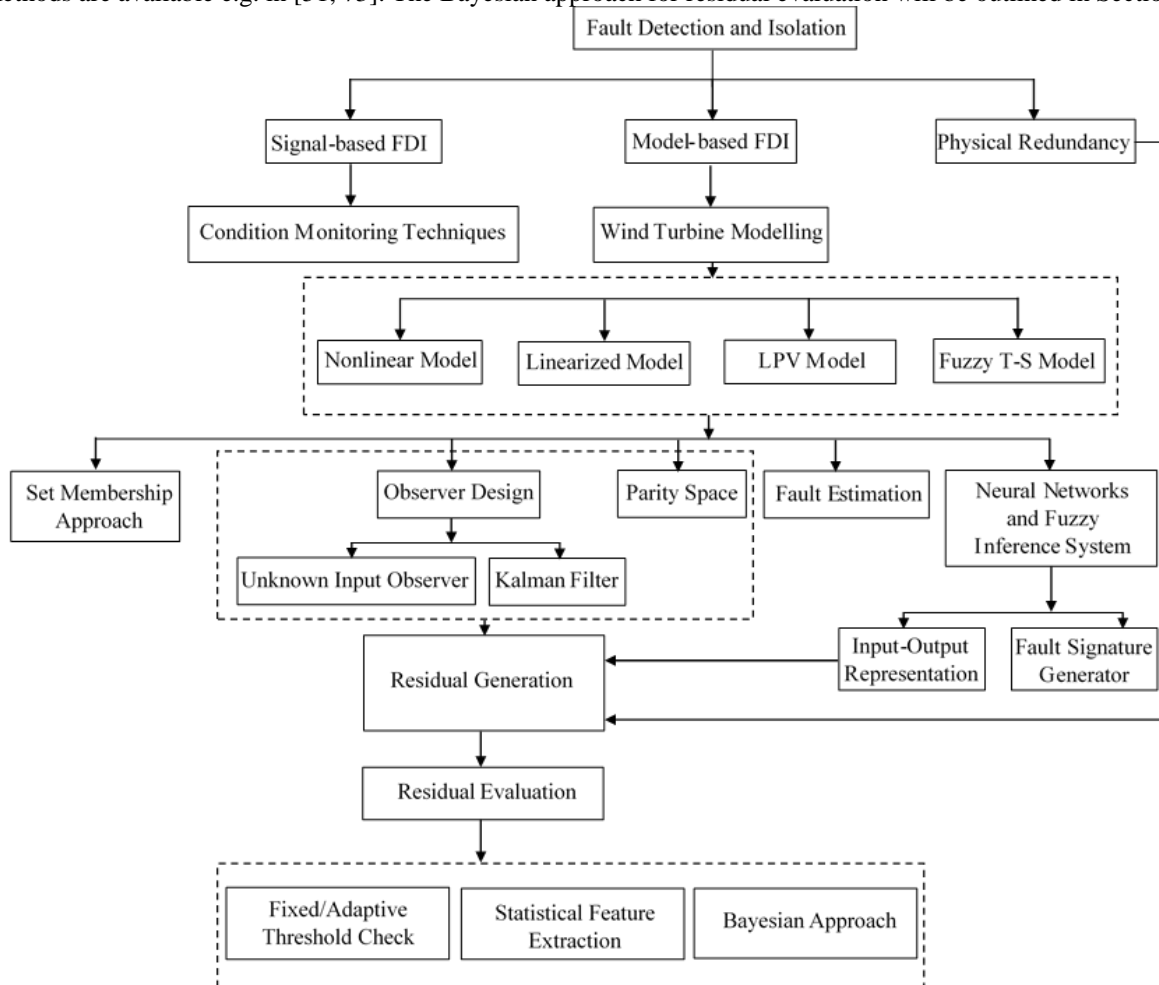


Fig. 4. FDI methods applied on wind turbines.

323
 324
 325

3.1.1. Parity space approach

327 The parity residual generation approach can be adopted on the whole or a single part of the wind turbine to achieve
 328 the FDI task. This approach uses the mathematical model of the wind turbine presented in Section 2. This model is
 329 fed with the same inputs as the wind turbine. In the fault-free case, both the wind turbine and the model, generate the
 330 same outputs. Accordingly, by comparing these two outputs the residual signal is constructed, which deviates
 331 considerably from zero in the case of fault occurrence. This approach is sketched in Figure 5 [69, 74]. As an example,
 332 in [75] the parity equations are utilized to detect and isolate faults in the blade pitch actuator and drivetrain. The highly
 333 nonlinear wind turbine dynamics and its variable operation points make a high-fidelity description of the whole wind
 334 turbine behavior difficult. Also, the design of different models for each subsystem may increase the complexity of the

335 final scheme. Also, the wind speed is not accurately measurable. Figure 5 highlights that the wind speed is one input
 336 to the wind turbine, which should be identically fed to the model. So, the wind speed should be either accurately
 337 measured or estimated. Different measurement or estimation of wind speed approaches have been reviewed in [76].
 338 On the other hand, in the case of offshore wind turbines, the unmeasurable sensor noise and environmental disturbance
 339 are considerable and inevitable. So, in [75] an appropriate filter was designed to make the residual robust against noise
 340 and disturbances, while yet being sensitive to the considered faults. Also, in [77] an adaptive threshold is designed to
 341 accurately evaluate the constructed residual signal of the wind turbine to eliminate false detection due to noise content
 342 on the residual.

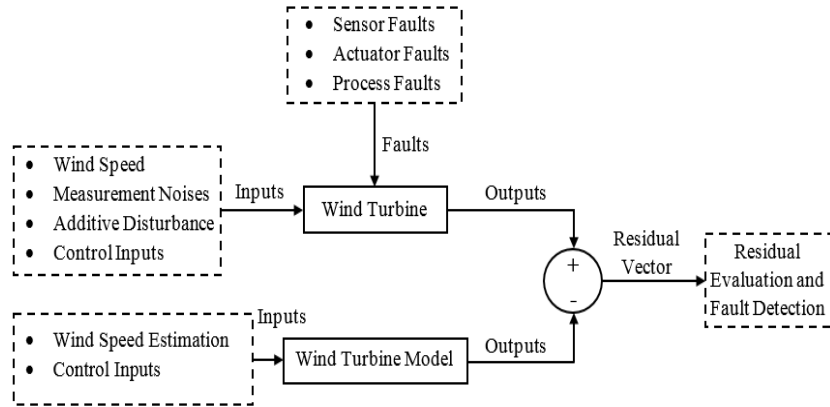


Fig. 5. Parity based residual generation approach.

3.1.2. Observer design approach

343
 344
 345 The most accurate residual generator is obtained by means of an appropriate fault diagnosis observer. Indeed, this
 346 approach relies on residual signals that are decoupled from the unknown inputs, whether wind speed, noises or other
 347 uncertainty effects [10]. In contrast to the parity approach, in the observer design, the observation error is fed back
 348 into the dynamic system to reduce the error, adopting a proper observation gain. Consequently, using the observed
 349 states, the residual signal is constructed. The observer is designed for the fault-free model. So, considering (10), the
 350 observer dynamic system is defined as,
 351

$$\begin{aligned}
 \dot{\hat{x}} &= A\hat{x} + Bu + R\hat{V}_r + He, \\
 \hat{y} &= C\hat{x}, \\
 e &= y - \hat{y},
 \end{aligned} \tag{15}$$

352 where, \hat{x} is the estimated wind turbine states vector, \hat{V}_r is estimated wind speed, \hat{y} is estimated outputs vector, e is
 353 observation error and H is the observer gain matrix. The only condition for the design of the observer is that the
 354 considered wind turbine model (or a part of it) must be observable, i.e. $rank([C \ CA \ \dots \ CA^{n-1}]^T) = n$, where $n =$
 355 $length(x)$. If the H is designed properly, e converges to zero. This approach is depicted in Figure 6, where the
 356 estimation of wind speed, i.e. \hat{V}_r is still required.

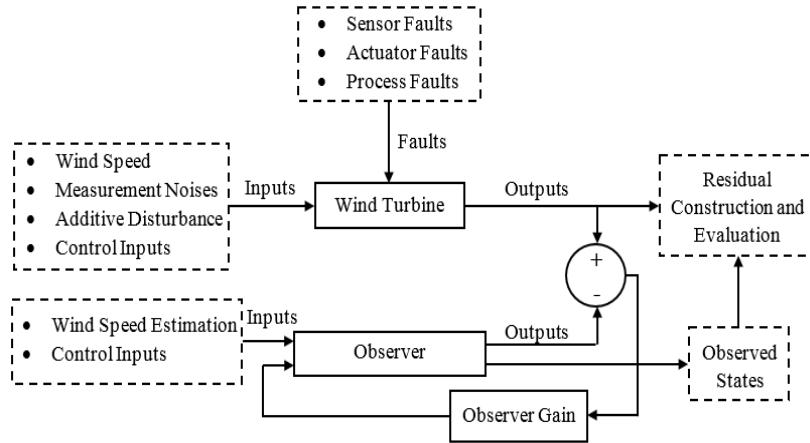


Fig. 6. Observer based residual generation approach.

357
 358 The wind turbine observer design mostly includes various types of Kalman filter [51, 78, 79] and unknown input
 359 observer (UIO) schemes [70, 80]. For example, using the Kalman filter, as the optimal observer, the reduction of wind
 360

361 turbine sensor noise on the observed states, is optimally guaranteed [51, 78, 79, 81]. The main disadvantage of the
 362 observer based FDI methods is that the whole linearized wind turbine model should be used to take advantage of well-
 363 developed linear observer design theories [3]. Recently the sliding mode observer has shown interesting results to be
 364 implemented on the whole nonlinear model of the wind turbine [82, 83]. In [84] the observer design is conducted on
 365 the wind turbine LPV model, which shows acceptable FDI performance for different fault scenarios. In [3], an
 366 extended observer on the wind turbine LVP model was designed to estimate system states and fault signals
 367 simultaneously. Also, via H_∞ optimization the robustness of the observer is improved against additive disturbances.
 368 Similarly, in [51], for disturbance decoupling and, meanwhile, to generate the optimal residual signal with respect to
 369 sensor noise, the Kalman filter is augmented with observers. A bank of several observers was proposed in [85], each
 370 of them being sensitive to only one fault and robust against the other faults. So, via the fault signature analysis, the
 371 fault detection as well as isolation are achieved at the same time. In [79] the performance of the Kalman filter, bank
 372 of observers and parity based residual generation are compared. It should be noted that in [27, 86] a new observer
 373 design scheme is proposed for wind turbine fault detection, known as interval observer design, for a set of valid models
 374 using the so-called set-membership approach.
 375 UIO represents an improvement of the ordinary observer scheme to eliminate the need for wind speed estimation. In
 376 UIO, the observer dynamic system is totally decoupled from external unknown disturbances, i.e. wind speed, by
 377 adopting a proper observer structure, which is given as,

$$\begin{aligned}\hat{\mathbf{z}} &= \mathbf{F}\mathbf{z} + \mathbf{T}\mathbf{B}\mathbf{u} + \mathbf{K}\mathbf{y}, \\ \hat{\mathbf{x}} &= \mathbf{z} + \mathbf{G}\mathbf{y}, \\ \hat{\mathbf{y}} &= \mathbf{C}\hat{\mathbf{x}},\end{aligned}\tag{16}$$

378 where, \mathbf{z} is the observer states vector, \mathbf{F} , \mathbf{T} , \mathbf{K} and \mathbf{G} are matrices to be designed for achieving the decoupling \mathbf{R} .
 379 Necessary and sufficient conditions for design of UIO are, $\text{rank}(\mathbf{C}\mathbf{R}) = \text{rank}(\mathbf{R})$ and $(\mathbf{C}, \mathbf{A}_1)$ is a detectable pair,
 380 where $\mathbf{A}_1 = \mathbf{A} - \mathbf{R}((\mathbf{C}\mathbf{R})^T \mathbf{C}\mathbf{R})^{-1} (\mathbf{C}\mathbf{R})^T \mathbf{C}\mathbf{A}$. In this scheme, the disturbance effect on the residual signal is decoupled.
 381 In [70, 80], the wind turbine sensor faults are detected with the UIO based approach.

382 3.2. Fault estimation approach

383 This approach relies on a proper fault estimator that is used for fault detection purposes. Also, an estimator bank can
 384 be designed to isolate the faults affecting different wind turbine components [42]. Each estimator of the bank is
 385 designed for a specific fault. The general estimator structure can be represented as,

$$\hat{\mathbf{f}} = g(\hat{\mathbf{f}}, \mathbf{y}, \mathbf{u}, \hat{\mathbf{v}}_r),\tag{17}$$

386 where, $\hat{\mathbf{f}}$ is an estimated fault and g is a nonlinear function to be designed. Despite the observer approach, in the
 387 estimation techniques, the fault function is directly obtained. The main step in the estimator design is the selection of
 388 design parameters. Indeed, in the case of proper design parameter selection, the need for the threshold is eliminated
 389 [42]. In Figure 7, the fault estimation is illustrated schematically. The estimator structure is designed as a dynamic
 390 system or static estimator such as the least squares filter [3, 87]. It should be noted that considering the nonlinear
 391 dynamics of wind turbines and different sources of disturbance, adaptive filters are mainly addressed by the most
 392 recent studies [32, 82]. The advantage of the adaptive estimator concerns its robustness, which can be theoretically
 393 guaranteed. This feature leads to reduction in the false and missed detection rates [29, 88]. The most recent fault
 394 estimator designs exploit fuzzy sliding mode estimators, whose application for wind turbines FDI is addressed in [82,
 395 89, 90].

396 3.3. Neural networks and fuzzy inference system approaches

397 Neural networks and fuzzy inference systems can be used for wind turbine FDI designs, and they are mainly divided
 398 into two different approaches, namely input-output representation and fault feature generators (classifiers), analyzed
 399 in the following sections.

400 3.3.1. Input-output representation

401 Neural networks provide one of the best tools to represent the nonlinear and partially known behaviour of wind
 402 turbines [48]. This approach is illustrated in Figure 8, in which the designed neural network is fed with the
 403 actual/estimated inputs, i.e. the same as the wind turbine, to generate the redundant outputs. It should be noted that
 404 the wind speed can be estimated in the neural network as well as the duplicated outputs [91, 92].

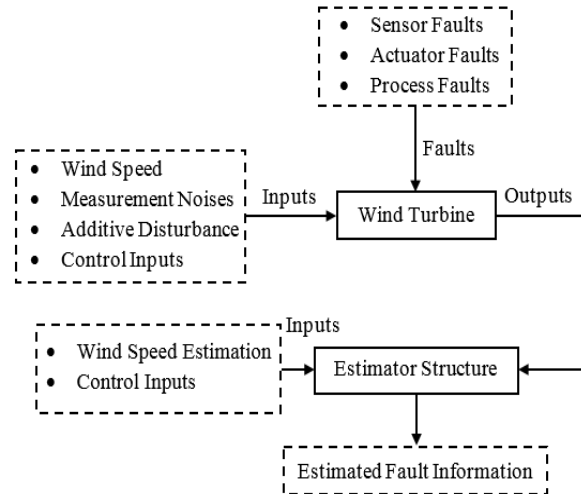


Fig. 7. Fault estimation diagram.

405
406
407
408
409
410
411
412
413
414

The multi-layer perceptron networks and radial basis function neural networks are the most commonly adopted structures for FDI purposes. The main step in this approach is the offline training to tune the neuron weights to the optimal ones. Adaptive neuro fuzzy interface system is an online fast learning adaptive training approach, which takes advantage of the neural network robustness, the learning and training capabilities, and the fuzzy inference system interpretability. In both offline and online schemes, a properly large dataset should be available as a-priori knowledge to train the network in the fault-free case. Accordingly, some works proposed a data-driven learning scheme [93]. The application of this approach on wind turbines FDI has recently been addressed in [94] and applied on different wind turbine components e.g. gearbox and generator faults [95, 96] and pitch faults [95].

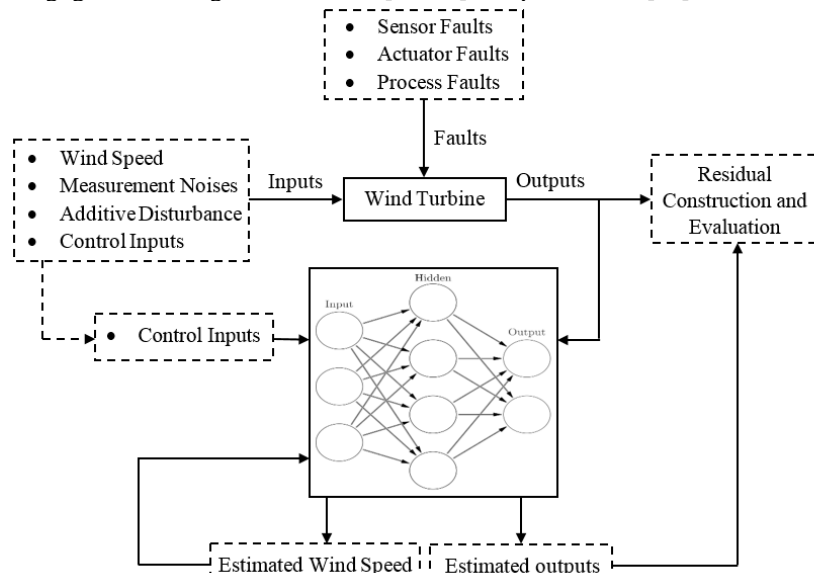


Fig. 8. Neural network input-output based FDI.

415
416
417
418
419
420
421
422
423
424
425

3.3.2. Fault signature generator

In contrast to the previous approach, the fault information can be directly extracted/inferred in this method, which relies on the design of an accurate a-priori knowledge-based network, e.g. Adaptive Neuro-Fuzzy Inference System (ANFIS) or Fuzzy Inference System (FIS), as illustrated in Figure 9. Accordingly, the expert knowledge is needed to be included in the design, whether as the numerical rules or fuzzy *if-then* linguistic rules. For example, the rule “*If generated power is high at low wind speed region, it may imply possible sensor fault*” can be used. These rules are also known as classifiers [97]. One of the advantages of fuzzy logic and fuzzy membership representation is that the uncertain measurement of the wind speed provided by the anemometer can be directly used [98]. In [99], classification methods are utilized for rotor imbalance/aerodynamic asymmetry fault detection.

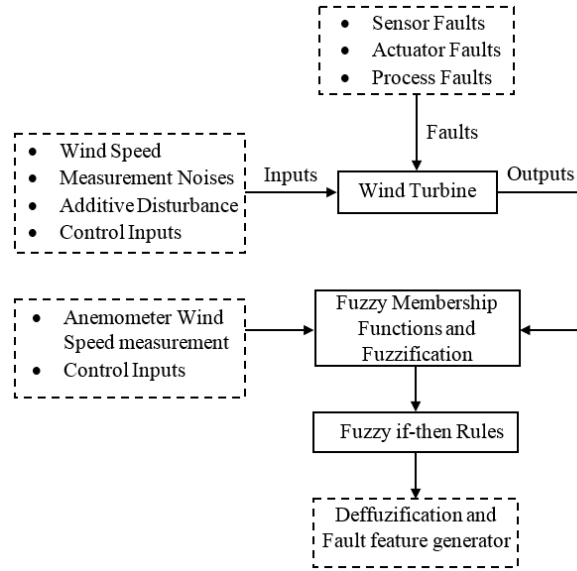


Fig. 9. Fuzzy fault feature generation diagram.

426
427

428 3.4. Set-membership approach

429 This scheme relies on a set of mathematical models of the wind turbine that are exploited for system consistency
 430 checking. Model uncertainties and noises are assumed to be unknowns, but with known upper and lower bounds. Due
 431 to unmodeled dynamics, noise and uncertainty of the wind turbine, the input/output data can be consistent with more
 432 than one model [100, 101]. So, an active model diagnosis is adopted in which, at each time step taking model
 433 falsification concepts into consideration, an auxiliary input signal is fed into both wind turbine and model sets, to find
 434 the correct model out of the predefined set. Then, the consistency of the current input/output data and the model is
 435 checked to detect the possible faults [71].

436 This method guarantees that the valid model of the wind turbine is never falsified. Additionally, the set-membership
 437 approach can be used only for one subsystem to check only one parameter, i.e. the feasible parameter set is defined
 438 instead of the valid model set [87, 102], assuming the wind speed and measurement noise are bounded as $|V_r| \leq V_{r,max}$
 439 and $\mathbf{D} \in \bar{\mathbf{D}}$ in (10) and (11). Also, initial conditions can be given in a compact set $\mathbf{x}(0) \in \mathbf{X}_0$. In every iteration of the
 440 set-membership algorithm, a consistent set, $S^c(t)$ is defined which contains all the states that are consistent with the
 441 wind turbine model, considering \mathbf{X}_0 , $V_{r,max}$ and $\bar{\mathbf{D}}$. The control input \mathbf{u} can be used for FDI purposes, but here, to
 442 significantly excite the wind turbine, assume that an auxiliary input $\mathbf{u}^a(t)$ is applied to the wind turbine. The predicted
 443 set S^p at time step t can be defined as $S^p(t) = \{\mathbf{Ax}(t-1) + \mathbf{Bu}^a(t-1) + \mathbf{R}\hat{V}_r(t-1) | \mathbf{x}(t-1) \in S^c(t-1), \hat{V}_r(t-1) \leq V_{r,max}\}$. Also, the updated set S^u at time step t can be defined as $S^u(t) = \{\mathbf{x}(t) | \mathcal{C}\mathbf{x}(t) \in \mathbf{y}(t) \oplus (-\bar{\mathbf{D}})\}$, where
 444 \oplus denotes the Minkowski sum. Now the consistent set can be computed as $S^c(t) = S^p(t) \cap S^u(t)$. A fault can then
 445 be detected at time step t if the following relation holds true,
 446

$$S^c(t) = \emptyset. \quad (18)$$

447 An advantage of the set-membership approach is that the need for thresholds is eliminated while the false alarm and
 448 missed alarm are avoided [86, 100]. The conservatism of this approach, because of uncertainty propagation and over-
 449 approximations required in the set computations, is the main drawback. This approach is illustrated in Figure 10. The
 450 combination of set-membership approach and observer design emerges as a new and promising approach for wind
 451 turbine FDI, as proposed in [27, 86].

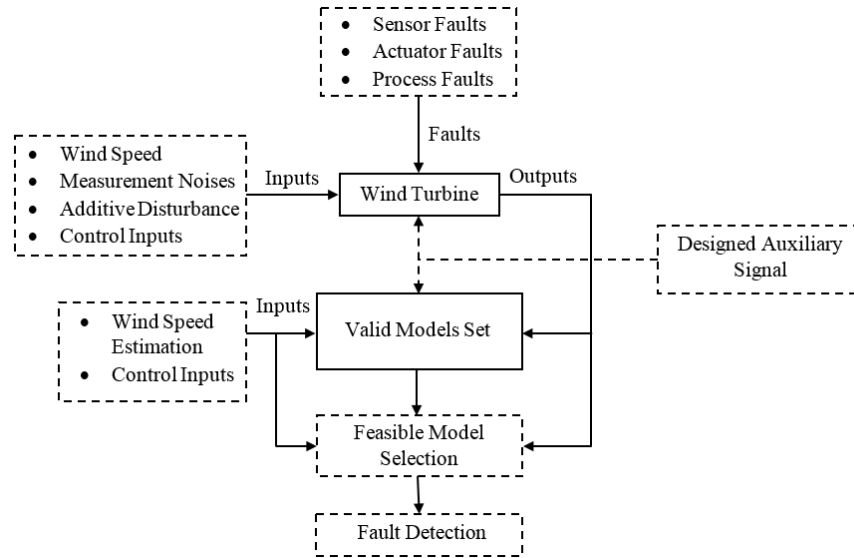


Fig. 10. Set-membership FDI approach.

452
453

3.5. Bayesian approach

455 This approach has recently been reformulated for model-based wind turbine FDI application [103], in contrast to its
 456 traditional application for signal-based condition monitoring. In this regard, in the Bayesian framework, the residual
 457 signal is evaluated to detect faults. By taking advantage of Bayesian reasoning, the expert knowledge about the wind
 458 turbine operation can be directly included in the FDI scheme [104]. Indeed, the residual evaluation is obtained as the
 459 fault probability extraction in the Bayesian framework as, $P(f|d, \hat{x}, y)$ i.e. the conditional fault probability having
 460 residual, estimated state and output vectors [105]. Accordingly, the need for threshold evaluation is eliminated. Also,
 461 using the valid measurement, a fault occurrence can be predicted, by considering Bayesian fault probability, e.g. wind
 462 turbine bearing crack prediction [106]. A recent and promising approach for the wind turbine feasible parameter set
 463 determination is addressed in [104] where the set-membership FDI is reformulated in a Bayesian framework.

4. Application of Fault detection methods to wind turbine components

465 In this section, the methods that have been introduced in Section 3 are analyzed and discussed based on their
 466 application on wind turbine components. The aim is to critically review the methods to enable the readers to choose
 467 appropriate methods for further study.

4.1. Sensor fault detection

469 As the sensor outputs are mostly utilized in the feedback controller scheme, the required wind turbine performance
 470 may not be maintained due to a fault on the corresponding sensor [10]. Especially in the case of the offshore wind
 471 turbines operating in harsh environment, it is more likely that the sensor measurements are corrupted with faults [68].
 472 The pitch sensor FDI is studied in [10], as the pitch angle control is a vital scheme for power regulation of wind
 473 turbines. The residual signal is generated using the physical redundant sensors and evaluated by considering mean and
 474 variance changes. In the parallel loop, the model-based pitch sensor is utilized to enable parity relation construction
 475 to isolate the detected fault. Indeed, it is aimed to identify which pitch sensor is faulty.

476 The application of the Kalman filter has been considered on wind turbine sensor FDI, in which it is guaranteed that
 477 the noise effect is minimized when proper conditions are satisfied. For example, in [68] the Kalman filter is designed
 478 for pitch sensor FDI. Similarly, in [51] the Kalman filter is used for the residual generation which is evaluated via the
 479 generalized likelihood ratio test to detect the pitch and drivetrain sensor faults, while the redundant sensor is needed
 480 for fault isolation. Also, the applied aerodynamic torque, i.e. T_a in (4), is considered as a disturbance and the designed
 481 Kalman filter has proven to be robust against wind speed variation.

482 The observer design has been analyzed in different modelling frameworks. For example in [44], the power sensor and
 483 generator speed sensors are considered and the observer is designed for the LPV wind turbine model, but the sensor
 484 noise is not considered. In [107, 108] H_2/H_∞ optimization is addressed to minimize the noise effect on the designed
 485 FDI observer. In [3], the extended observer for the whole wind turbine model is designed in the LPV framework to
 486 estimate the states as well as faults at the same time for pitch and drivetrain sensor faults using the linear matrix
 487 inequality. So, this approach can be considered as an estimation method. Also, the wind speed is considered as an
 488 unknown disturbance and the proposed observer is insensitive to it. The fuzzy T-S framework has been considered in
 489 several papers to design the sensor FDI scheme. In [109] for low wind speed regions and in [29] for high wind speed

490 regions, the generator current sensor fault is detected via an observer design in the fuzzy T-S framework. Similarly,
 491 in [110], [111] and [112], the generator voltage sensor, pitch sensor and generator speed/power sensors, respectively,
 492 are considered and fuzzy T-S fault observers are designed.
 493 Regarding the unknown wind speed variation, UIO design is an appropriate choice to remove the need for wind speed
 494 estimation, especially considering drivetrain sensor FDI designs [85]. In this approach, the wind speed variation is
 495 decoupled from the designed observer [80]. For example, in [70, 80, 113] UIO is designed for drivetrain sensor fault
 496 detection including rotor speed and generator speed sensors. Observer bank design is a suitable approach to detect and
 497 isolate the sensor faults, and at the same time, to achieve fault isolation with no need for physical redundant sensors.
 498 Each observer is designed to be sensitive only to one given fault and robust to other faults and disturbances. In [85],
 499 the UIO bank is designed for a set of sensor faults including rotor speed, generator speed and wind speed sensors.
 500 Finally, more accurate evaluation of the residual signal can be conducted with set-membership checks or Bayesian
 501 inferences. In [100], the pitch and rotor sensor faults are considered and, utilizing the set-membership approach, the
 502 need for threshold checking is removed and also, no positive false alarm is produced. In [103] the relationship between
 503 wind turbine failure root causes and symptoms are used with a Bayesian Network for pitch sensor fault detection,
 504 using SCADA data to reduce false alarms and missed fault rates. The available wind turbine sensor FDI methods
 505 associated with different fault sources, are analyzed comprehensively in Table 5.
 506

Table 5. Wind turbines sensor FDI methods.

Fault Source	FDI Method	Reference	Advantage	Disadvantage
Pitch Sensor	Physical Redundancy/ Parity Equation	[10]	Accurate fault detection. No need for wind speed estimator.	Need for extra physical pitch sensors.
	Observer (H-/H ∞ Optimization)	[108]	Noise effect reduction on residual.	Need for wind speed estimation. Complex and timely numerical algorithm.
	LPV Extended Observer	[3]	Estimation of the states as well as faults at the same time.	Sensitive to design parameters. Complex procedure for computer simulation.
	Kalman Filter Design	[51, 68]	Minimization of noise on residual.	Wind speed estimation. Complex and timely numerical algorithm. Need for an extra sensor for isolation.
	Fuzzy T-S Observer	[111]	More accurate wind turbine model. The reduction of modelling uncertainty on the fault detection.	The effective design of fuzzy rules and set-memberships.
	Set-Membership Approach	[100]	Threshold check is not needed. No positive false alarm is produced.	Wind speed estimation. Need for implementable and simplified numerical algorithm to calculate the valid models set.
	Bayesian Inference using SCADA data to generate fault symptoms	[103]	Reduced false alarm and missed fault rates.	Considerable sensor noise effect. Low sample rate of SCADA data.
Drivetrain Sensors	Kalman Filter Observer	[51]	Aerodynamic torque is considered as disturbance. Minimization of noise on residual.	Complex and timely numerical algorithm. Need for an extra sensor for isolation.
	LPV Extended Observer	[3]	Estimation of the states as well as faults at the same time. No need for wind speed estimation.	Sensitive to design parameters. Complex procedure on digital computer.
	UIO	[70, 80, 113]	One-step calculation design procedure.	Too simplified modelling assumptions in the design which make it less practical.
	UIO Bank	[85]	Fault detection and isolation at the same time.	
	Set-Membership Approach	[100]	Threshold check is not needed. No positive false alarm is produced. Less complex computational procedure.	Need for wind speed estimation.
Generator Voltage and Current Sensors	Observer	[114-116]	No need for any extra redundant sensor.	Effect of sensor noise content on the observation performance is not considered. Need for wind speed estimator.
	Fuzzy T-S Observer	[29, 109, 110, 112]	More accurate wind turbine model. The reduction of modelling uncertainty on the fault detection.	The effective design of fuzzy rules and set-memberships.
Power Sensor	Observer (H-/H ∞ optimization)	[107]	Noise effect reduction on residual.	Wind speed estimation. Complex and timely numerical algorithm.
	LPV observer	[44]	Observer design for whole wind turbine.	No noise/disturbance consideration.

507 **4.2. Pitch actuator fault detection**

508 The power regulation of wind turbines is essential for high wind speed situations, i.e. to retain the generated power at
 509 nominal power, by adjusting the blade pitch angle to control the applied aerodynamic torque and consequently, rotor
 510 speed [34]. Also, in dangerous wind speed situations, it is aimed to feather the wind turbine by pitching the blades
 511 into the desired orientation to bring the wind turbine to a stop, to avoid mechanical brake engagement, which may
 512 induce considerable stress on the rotor shaft. So, the pitch actuator plays a vital role to accurately tune the blade pitch
 513 angle at β_{ref} . Accordingly, the pitch actuator faults lead to deviation of the pitch angle from β_{ref} . As the pitch actuator
 514 fault-free dynamic behavior (5) is represented as a linear and known relation, the parity equation can be used to
 515 generate the residual. As the measured pitch angle, to be used in the parity equation, is corrupted by measurement
 516 noise, in [117] the least square residual evaluation with sliding data window is exploited to evaluate the residual signal
 517 and detect $\Delta\tilde{f}_{PAD}$ while minimizing noise effects. On the other hand, $\Delta\tilde{f}_{PAD}$ can be considered as the model uncertainty
 518 and accordingly, in [75] the robust residual filtering and parity equations are combined to accurately detect the pitch
 519 actuator dynamic change for each blade. Also, the pitch sensor fault effect is distinguished from $\Delta\tilde{f}_{PAD}$, utilizing the
 520 fault-end-effect, i.e. fault signature.

521 The pitch sensor noise, dynamic change and bias are challenging effects to be separated at the same time, which
 522 motivates many recent studies, for which observer design is a potentially suitable approach. In [118] the Kalman filter
 523 observer is designed to detect the pitch actuator bias. Also, in [108], the $H/H\infty$ optimization method is augmented in
 524 the observer design to generate the optimal residual, i.e. minimizing the noise effect. Regarding pitch sensor effects,
 525 in [84] an observer is designed with adaptive gains to detect dynamic change, distinguished from sensor noise and
 526 sensor faults. In a similar manner, in [32], the sliding mode observer is designed to detect dynamic change with an
 527 adaptive hierarchical method to facilitate the real-time implementation. In [82], the sliding mode observer is designed
 528 for the wind turbine fuzzy T-S model to detect any increased time delay in the electrical pitch actuator.

529 The application of soft computing using SCADA data to detect pitch actuator faults have shown promising results to
 530 avoid complicated FDI schemes. In [95] using neural networks, a pattern recognition structure was proposed to detect
 531 pitch actuator faults. On the other hand, in [94] the Bayesian fault probability was obtained to evaluate the SCADA
 532 alarm data and detect potential pitch actuator dynamic change. To this end, pitch actuator FDI methods are elaborated
 533 in Table 6.

Table 6. Pitch actuator FDI methods.

Fault Type	Fault Symbol in (6)	Fault Detection Method	Reference	Characteristic	Advantage	Disadvantage
Pitch Actuator Dynamic Change	$\Delta\tilde{f}_{PAD}$	Parity Equation	[117]	Least square residual evaluation with sliding data window.	Minimizing noise effect and accurate fault size estimation.	Pitch sensor fault effect and pitch bias are not considered.
			[75]	Robust residual filtering.	Considering both pitch sensor and pitch actuator dynamic change.	No sensor noise is considered.
		Observer Design	[108]	$H/H\infty$ optimization method.	Optimal residual sensor noise attenuation.	
		Observer Design	[84]	Adaptive observer gains.	Sensor noise and sensor faults are considered. Adaptive observer is only sensitive to dynamic change.	Sensitive to design parameters. Complex procedure using computer simulation.
			[32]	Sliding mode observer.	Facilitate the real-time implementation.	
		Bayesian fault probability	[94]	Evaluation of the SCADA alarm data.	Reduced false alarm and missed fault rates.	Sensor noise and faults are not considered. The low sample rate of SCADA data.
		Neural networks	[95]	A pattern recognition structure.	Robustness against sensor noise and model uncertainty.	No sensor fault is considered.
Pitch Actuator Bias	β_{bias}	Observer Design	[118]	Kalman filter observer.	Good sensor noise attenuation	Pitch actuator uncertainty and dynamic change are not considered.
Electrical Pitch Actuator Time Delay Change	-		[82]	Sliding mode observer fuzzy T-S model.	More accurate wind turbine model. The reduction of modelling	The effective design of fuzzy rules and set-memberships. Sensitive to design parameters.

					uncertainty on the fault detection.	
--	--	--	--	--	-------------------------------------	--

535 **4.3. Generator and converter fault detection**

536 The Maximum Power Point Tracking (MPPT) of variable speed wind turbines is achieved by regulating the electrical
 537 generator torque using converter current control. The generator torque control leads to adjustment of the generator
 538 and rotor speeds to the desired values such that consequently, the power coefficient C_p is maintained at the maximum
 539 possible one. Accordingly, the generator faults including bias f_{T_g} and dynamic change $\Delta \tilde{f}_{GC}$ cause the deviation of
 540 operation from the intended one. So, it is important to detect and isolate the generator faults. The large variety of wind
 541 turbine manufacturers inevitably results in different manufacturer-specific wind turbine generator technology [119].
 542 Accordingly, it is fruitful to consider the generator FDI methods in the system control level, for the various different
 543 electrical generator topologies, as outlined in this section. The available FDI methods for the generator bias are
 544 summarized in Table 7.

545 In [44], a wind turbine LPV model, including uncertainty, uses a LPV observer designed to generate the residual, and
 546 adopting the adaptive threshold method the generator torque bias is detected. In [79] three different generator FDI
 547 schemes are considered. In the first scheme two cascade Kalman filters are utilized for mitigation of the nonlinear
 548 aerodynamic torque effect. In the second scheme, a bank of dedicated observers is exploited. The third scheme is
 549 designed using a H_∞ filter with parity equations, by considering the nonlinearity as a bounded disturbance. Also, in
 550 [120], by adopting interval observers and considering the noise and modelling errors as bounded unknowns, the
 551 generator fault is detected using online analysis of observed fault signatures and comparing them with the theoretical
 552 ones obtained using structural analysis. The fault size is estimated based on the batch least squares approach.

553 The parity relation, using analytical redundancy relations and interval observers, for uncertain wind turbine model,
 554 was developed in [27]. On this basis, using the set-membership approach, the generator bias is accurately detected.
 555 Similarly, in [100, 121], a consistent set with measurements is generated using the set-membership approach. Model-
 556 reality mismatch, noise, and uncertainties on the torque coefficient and generator fault are included in the wind turbine
 557 model. An effective wind speed estimator is proposed. For representing the consistent set of models with
 558 measurements, a matrix zonotope is used, which results in a computationally efficient scheme. The results confirm
 559 the effectiveness of the proposed method compared to other methods for the same fault scenario. The approach does
 560 not need to use threshold design, which is an outstanding advantage of the proposed method.

561 In [14], the fuzzy theory is exploited to manage uncertain models and noisy data. The residual signals, which are only
 562 sensitive to generator faults, are generated using fuzzy T-S prototypes. The data-driven diagnosis strategy, based on
 563 fuzzy T-S prototypes is proposed in [45] for converter FDI with generator and sensor faults. The reliable regulation
 564 of the generator torque, including both generator uncertainties and faults, is studied in [20], and two different schemes
 565 are developed. Firstly, a FIS is proposed for parameter adaptation, without any prior knowledge of the generator faults.
 566 In the second approach, the fuzzy T-S identification approach was exploited, to develop an integrated FDI scheme to
 567 detect potential generator faults using online diagnostic information. The adaptive fault estimation is exploited in [42]
 568 for generator and converter FDI. Also, in [29] a two-dimensional polynomial is suggested to estimate the power
 569 coefficient in an analytical form. Consequently, the adaptive filter is obtained via the nonlinear geometrical approach
 570 to detect the generator faults.

571 **4.4. Drivetrain fault detection**

572 The drivetrain can be subjected to changes in its dynamics modeled as ΔK_{dt} and ΔB_{dt} in (4), which may happen very
 573 slowly. It causes undesirable oscillations, which may lead to total breakdown which causes long and costly downtime
 574 [17]. So, it is important to detect this fault in time. It should be noted that most of the developed FDI methods applied
 575 to the drivetrain are considered as signal-based approaches [95], where significant literature reviews can be found in
 576 [4, 21-24, 65]. Accordingly, this section considers only the model-based FDI methods. In [75] the parity relation is
 577 designed on the drivetrain to generate the residual signal and, via robust filtering the residual signal is evaluated to
 578 detect changes in drivetrain dynamics. Also, the wind speed is used in the structure of parity relation assuming that
 579 the wind speed estimation is separately available, and it is not affected by the fault occurrence which is generally not
 580 true. On the other hand, the measurement noise is not considered. Accordingly, in [81] the Kalman filter is utilized to
 581 minimize the noise effect and detect the drivetrain efficiency loss due to wear and increased gear friction. The dynamic
 582 change may be considered as the change in the resonance frequency and damping ratio of the drivetrain. In this regard,
 583 in [41], this change is detected by designing a filter and using only the generator speed measurement. The uncertainties
 584 of the drivetrain dynamic response, i.e. unknown aerodynamic torque T_a in (4), and high sensor noise, have led to the
 585 development of more advanced FDI solutions. In [96], a neural network was designed for drivetrain FDI by training
 586 the network with a large amount of fault-free data to attenuate uncertainty and noise effects. Also, in [90, 122], utilizing
 587 fuzzy T-S prototype modelling, the drivetrain fault was detected by designing a sliding mode observer with adaptive
 588 gain. Also, the fault size was identified using an equivalent output injection method.

589 **4.5. Aerodynamic characteristic change detection**

590 Debris build-up and blade erosion reduces the blade aerodynamic efficiency, as can be seen in (3). As a result, the
 591 captured aerodynamic torque and power are decreased. Also, the uneven oscillation of blades is a reported issue of
 592 this change [123]. Furthermore, the power regulation by blade pitch angle adjustment is not satisfactorily achieved.
 593 So, it is very important to foresee the aerodynamic characteristic change in the controller design and to detect this
 594 potential change. This change is difficult to detect because it is challenging to determine if reduced power generation
 595 is due to the blade debris/erosion, or if the wind speed has dropped [124]. Also, as debris build-up happens slowly, it
 596 is mostly assumed that this change lies within the annual wind turbines maintenance/inspection and the blades are
 597 cleaned/replaced. So, the literature focusing on this change is still limited. In [100], the blade aerodynamic change is
 598 described as the uncertainty on the torque coefficient. Accordingly, a consistent set of models is generated using
 599 measurements and the nominal wind turbine representation, which includes uncertainties and noise, and by means of
 600 the set-membership approach. This set includes all possible states consistent with the fault-free system. If the current
 601 measurement is not consistent with this set, a fault is detected. Also, it is stated that when the torque coefficient change
 602 is introduced, some faults are not detectable. Consequently, in [25, 125] instead of the individual wind turbine FDI,
 603 the blade debris build-up and erosion are detected at the wind turbine farm level and it is shown that this change is
 604 easier to be detected at this scale. This is achieved by comparing the output powers of the wind turbines operating
 605 under almost the same wind conditions. The nonlinear wind turbine model is obtained by fuzzy T-S modelling. Also,
 606 the FDI scheme comprises a rule-based threshold test logic for residual evaluation.

Table 7. Generator bias FDI methods.

Fault Detection Method	Reference	Characteristic	Advantage	Disadvantage
LPV observer based residual generation	[44]	LPV model of wind turbine including uncertainty and adopting the adaptive threshold.	Missed/false alarms are reduced.	Sensitive to design parameters. Complex procedure on Simulation.
Cascade Kalman filters/ observers bank/ H_∞ filtering using parity equations	[79]	Three different detection schemes are compared.	Nonlinearity is considered, and bounded uncertainty is attenuated.	Generator sensor fault is not considered in the proposed scheme.
Interval observers design.	[120]	Observed fault signatures are matched with theoretical ones using structural analysis. Fault size estimation using batch least squares.	Unknown and bounded noise and modelling errors are considered.	Overly simplified modelling assumptions in the design which makes it less practical.
Set-membership approach	[27]	Analytical redundancy relations and interval observers.	Unknown and bounded uncertain wind turbine nonlinear model is considered	Complex procedure for implementation.
	[100, 121]	Model of the wind turbine including uncertainties, noise, uncertainties on the torque coefficient and generator fault.	Effective wind speed estimator is proposed. Matrix zonotope is used to reduce computational complexity. No need for threshold design	The generator sensor noise is not considered.
Fuzzy T-S residual generation	[14]	Approximating uncertain nonlinear wind turbine models with fuzzy theory.	Managing noisy data. Residual is sensitive only to generator faults.	The effective design of fuzzy rules and set-memberships. Sensitive to design parameters.
	[45]		Detection and isolation of both generator/converter actuator and sensor faults.	
Fuzzy inference mechanism/ fuzzy T-S identification	[20]	Parameter adaptation without any knowledge of generator faults. Integrated fault detection.	Considering both uncertainties and faults on the generator.	
Adaptive fault estimation	[29]	Nonlinear geometric approach	A two-dimensional polynomial is suggested to estimate the power coefficient analytically.	The sensor noise is not considered.

608 **5. Fault-tolerant control of wind turbines**

609 FTC schemes are designed to maintain acceptable performance and stability of the wind turbines as close as possible
 610 to the fault-free conditions when faults occur, and to reduce the need for unplanned costly maintenance and unwanted
 611 shut downs. FTC techniques are divided into two different schemes, i.e. active and passive. The main difference is
 612 that active FTC needs the timely and accurate FDI information to be fed into the controller structure. Also, FDI
 613 information can be used in subsequent prescheduled maintenance plans. In contrast, in passive FTC, the controller is
 614 designed to be robust against a set of presumed faults. The benefit of the passive approach is that the controller is
 615 fixed and neither fault detection nor controller update are needed. However, some performance degradation in faulty
 616 conditions is tolerated. Stability is not necessarily guaranteed for the faults other than the considered ones [34].

617 The wind turbine power control objectives are defined based on the wind speed, which should be considered in FTC
 618 design. For the wind speed less than a given lower value, i.e. cut-in wind speed $V_{r,cut-in}$, the available wind power is
 619 not economical enough to overcome the operational cost, so the wind turbine is not put into operation. Also, for the
 620 wind speed greater than a given upper value, i.e. cut-out wind speed $V_{r,cut-out}$, the wind turbine is pitched-to-feather
 621 or braked to protect it structurally, despite the high available wind power. The region from $V_{r,cut-in}$ to the rated wind
 622 speed, i.e. at which wind turbine starts producing its rated power, is called the partial load region. Also, the region
 623 from the rated wind speed to $V_{r,cut-out}$ is called the full load region. In the partial load region, it is aimed to capture
 624 as much power as possible from the wind by controlling the generator torque, i.e. design of $T_{g,ref}$ in (8) and keeping
 625 the pitch angle at its optimal value, at which the $C_p(\beta, \lambda)$ curve is maximized. In the full load region, the aim is to
 626 make the wind turbine produce only its rated power, by controlling blade pitch angle, i.e. design of β_{ref} in (6) and
 627 fixing the generator torque at its rated value. In both regions it is desirable to minimize mechanical stress and actuator
 628 usage [21]. Also, a scheme is needed for bumpless switching between the controllers in the partial load and full load
 629 regions, due to possible inconsistency between controller signal magnitude at the switching time. Otherwise, a bump
 630 in the control signal may cause oscillations between the two controllers and consequently, make the wind turbine
 631 unstable. Finally, it is crucial to mitigate the structural loads in the design of the baseline controller. Indeed, the loads
 632 considerably reduce the wind turbine's lifespan. The most harmful loads appear in the full load region, in which drag
 633 and thrust loads on the wind turbine's structure are considerable, including the tower fore-aft vibration and the blades
 634 flap-wise oscillation. The aerodynamic torque variation leads to considerable torsional vibration of the drivetrain shaft.
 635 So, it is very useful to implement a drivetrain/tower stress damper module to dampen torsional/fore-aft vibrations,
 636 respectively. For instance, the filtered generator speed and power can be added to the generator torque and the pitch
 637 angle, respectively, to filter out the resonant frequency of the drivetrain/tower. Also, the asymmetrical torsional
 638 torques can be reduced via the individual blade's pitch control [20]. Note finally that a comprehensive review on the
 639 wind turbines baseline controllers design are available in [35, 126] and not reviewed here.

640 **5.1. Passive fault tolerant control methods**

641 In passive FTC design the controller is optimized for the fault-free case and some degraded performance is guaranteed
 642 when some presumed faults occur. The problem is formulated in the following form:

$$643 \quad u(t) = \arg \text{Opt}_{u \in U} \left(\begin{matrix} H \\ f \in F, D \in \bar{D}, V_{r,cut-in} \leq V_r \leq V_{r,cut-out} \end{matrix} \right), \quad (19)$$

644 where, H is the operational objective index, to be optimized, e.g. maximizing the extracted power, minimizing induced
 645 structural stress, drivetrain oscillation and actuation effort. So, this optimization problem involves finding the
 646 appropriate control $u(t)$ which belongs to the achievable control U . The considered faults f are in the given presumed
 647 faults set F and the applied disturbances D is bounded by \bar{D} .

648 In [33, 43, 127], a wind turbine LPV model in the full load region is considered, whilst the controller is designed to
 649 be robust against parameter variations, caused by nonlinear aerodynamics and against pitch actuator faults. Also, it is
 650 shown that the designed passive FTC has better performance than an industrial PI controller. In [128] a fuzzy-based
 651 framework including *if-then* rules, is presented to regulate both pitch angle and generator torque while adding fault
 652 tolerance features to the wind turbine in a passive way. Pitch and generator sensor faults, pitch dynamic change and
 653 generator torque bias were considered. In [129] a novel adaptive PID-based fault-tolerant controller with a Nussbaum-
 654 type function is proposed to be insensitive against unexpected pitch actuator faults, including pitch actuator bias and
 655 effectiveness loss.

655 **5.2. Active fault tolerant control methods**

656 Active FTC can be solved via the Virtual Sensor and Actuator (VSA) approach or the Controller Reconfiguration
 657 (CR) scheme. In VSA, the fault information identified from the FDI scheme, is fed into a virtual (software)
 658 sensor/actuator module, which is placed between the actual sensor/actuator and the baseline controller, to correct
 659 signals in the virtual sensor/actuator such that the fault effect is removed. In VSA, the baseline controller is still in
 660 operation, which is an interesting industrial aspect because the existing baseline controller needs no modification [87].
 661 For some faults, e.g. system faults in Table 4, the fault effects cannot be accommodated via VSA. Accordingly, in the
 662 CR approach the whole/part of the baseline controller is reconfigured to an alternative controller to guarantee stability
 663 and satisfactory performance. The CR is obtained by either modification of the current baseline controller parameters,
 664 switching a new controller, or using the available hardware/software redundant components [130, 131]. CR approach
 665 has less industrial acceptability due to its complex implementation, but it shows promising performance for the severe
 666 faults. The VSA and CR fault accommodations are illustrated schematically in Figure 11.

667

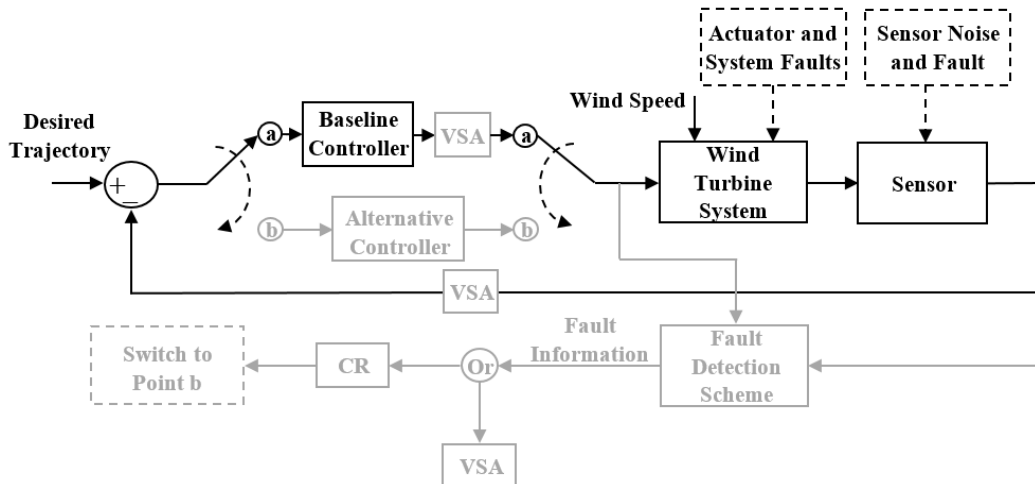


Fig. 11. VSA and CR fault accommodation (grey line) on the wind turbine (black line).

668
669

5.2.1. Virtual sensor/actuator faults accommodation

VSA is mostly applied to the wind turbine sensors, because the actuator signal correction may lead to instability, due to inaccurate fault size identification [120]. Also, it is easier to implement the virtual sensor module in practice. In [132] this technique is used to remove the drivetrain sensor faults. Similarly, in [87], VSA is used for pitch and drivetrain sensor faults, including both biased and gained sensor outputs, in which the set-membership approach is used to detect faults. Also, the generator torque bias is accommodated. In [133] using a similar approach, the drivetrain decreased efficiency due to dynamic change is additionally detected and accommodated. Also, in [14], different fault types, including fixed and gained pitch sensor, drivetrain sensors, generator torque offset, drivetrain changed dynamics and pitch actuator dynamic change are considered. In [90], a fuzzy T-S sliding mode observer is designed to estimate and consequently compensate the actuator faults by modifying the controller output via the virtual actuator. In [3] the pitch sensor fault and pitch actuator dynamic change are estimated through the design of an adaptive extended observer for an LPV wind turbine model. The PI industrial controller is used as the baseline controller and its output is corrected with the estimated fault information. Also, the robustness against wind speed variation and model uncertainty is guaranteed by H_∞ optimization. In [134], the fuzzy T-S model is used to design an extended state observer, the drivetrain sensor bias is detected and accommodated by correction. The corrected signal is fed into a T-S fuzzy dynamic output feedback controller to maintain the desirable performance. In [29] the proposed scheme exploits a robust actuator fault estimation approach based on adaptive filters. The considered faults are pitch actuator dynamic change, bias and generator torque bias. Accordingly, the output of the PI controller is corrected based on the estimated fault information. Finally, in [25], through the use of expert-generated fuzzy *if-then* rules, the generated power of each wind turbine in the farm is evaluated to detect the possible debris build-up. Accordingly, the generator torque is corrected in the VSA module to compensate for the debris build-up effect and to keep the generated power at the desirable value. It is worth noting that in the VSA the sensor faults are reasonably accommodated better than the system and actuator faults [26].

5.2.2. Controller reconfiguration

Considering the available CR methods, it can be stated that the process and actuator faults are better accommodated [26]. In [135] a group of model predictive controllers are designed to accommodate the pitch actuator dynamic change. A Kalman filter is used to identify the faults, and when detected, an alternative predefined controller is used to compensate for their effects. In [130], modified Ziegler-Nichols rules are applied to the online adaptive controller, relying on the least squares method with adaptive directional forgetting factors, to recursively adjust the PI baseline controller parameters to remove both generator and pitch actuator fault effects. In [136], a FTC scheme is proposed as a combination of model reference adaptive control with neural network compensation. Although, the fault is considered as a bounded additive actuation signal, however, no physically meaningful fault is considered. In [131], a proportional multiple integration observer is designed in the fuzzy T-S framework to estimate the generator sensor faults. Also, a robust estimation of effective wind speed is given. These estimations are used to compensate for the fault effects using a fuzzy T-S dynamic output feedback controller. In [112, 122], by deploying a robust fuzzy scheduler and multi fuzzy observers, a nonlinear wind turbine controller is designed to attenuate the sensor faults, actuator faults and parameter uncertainties on the overall performance. It is desirable to reconstruct and compensate several actuator faults with one observer. In this regard, the sliding mode controller design technique is advantageous.

707

708 An adaptive sliding mode observer is designed in [32] to estimate the pitch actuator dynamic change and to modify
 709 the traditional PI baseline controller for fault effect compensation. In [34] by combining a disturbance compensator
 710 with a controller in the discrete-time domain, pitch actuator FTC is developed. Fault estimation and discrete-time
 711 controller designs are simultaneously fulfilled using the disturbance compensator. In [127], the additional redundant
 712 pitch, rotor and generator sensors are considered in the proposed controller, to be deployed when fixed/no
 713 corresponding sensor outputs are detected. Recently, adaptive control has been used to deal with the faults, as a
 714 category of the active/passive combination method. Although, it may be dangerous practically, since this method may
 715 mistakenly accommodate faults, for example in critical fault situations, which requires a safety stop of the wind
 716 turbine. Accordingly, if the adaptation laws are designed accurately using expert's knowledge, the need for CR is
 717 removed to have a simple practical controller similar to passive FTC, and meanwhile, the FDI information is obtained
 718 which can be used to improve the maintenance schedules. On the other hand, no presumed fixed fault sets are needed,
 719 similar to active FTC. In [31, 92] adaptive laws are defined as a part of the proposed controller to be used in the
 720 controller structure and to compensate for the actuator fault effects. In [31] the actuator fault is considered as an
 721 additive bounded disturbance, while in [92], pitch actuator dynamic change, pitch bias and generator torque bias are
 722 considered. To this end, in Table 8 the available FTC techniques are summarized.

723 **6. Discussion and Future studies**

724 Wind turbine FDI and FTC have recently emerged to support reliable wind power generation. Different FDI schemes
 725 are available, which can rely on the accurate modelling, among which fuzzy T-S and LPV are common descriptions.
 726 However, it is always desirable to design FDI schemes for the nonlinear model. Effective fault detection is the main
 727 step in the active FTC, so it should be well matured before practical implementation. This literature survey highlighted
 728 that the focus was on the FDI of the drivetrain and the pitch angle sensors, as these measurements are used in the
 729 feedback control system. Table 5 shows that observer design techniques are often used for sensor FDI. The diagnosis
 730 of pitch actuator and generator faults require FDI techniques outlined in Tables 6 and 7, respectively, which show that
 731 fault observers remain the best solution. Model-based FDI methods applied to the drivetrain are still limited since
 732 signal-based methodologies are mostly exploited. The blade aerodynamic change due to debris build-up and erosion
 733 can be detected more accurately at the farm level, compared to the individual wind turbine scale.
 734

Table 8. Wind turbine FTC techniques.

		Fault Tolerant Control Method			
		Passive	Active		
			VSA Approach	CR Approach	
Fault Source	Sensors	Pitch sensors	Fuzzy T-S multimodel and fuzzy if-then rule-based controller [128].	Set-membership approach [87]. Residual signal generated via fuzzy T-S model [111]. Fuzzy T-S residual generation [14]. Adaptive extended state observer [3].	Robust fuzzy scheduler [112]. Multi-observer switching control [122].
		Drivetrain sensors	-	Set-membership approach [87]. Residual signal generated via fuzzy T-S model [111]. Fuzzy T-S residual generation [14]. Fuzzy T-S extended state observer [134].	Multi-observer switching control [122]. Fuzzy T-S Dynamic Output Feedback Controller [131].
		Generator/ Converter sensors	Fuzzy T-S multimodel and fuzzy if-then rule-based controller [128].	-	-
	Pitch actuator	LPV wind turbine model, robust LMI-based controller [33, 43]. Fuzzy T-S multimodel and fuzzy if-then rule-based controller [128]. Adaptive PID-based controller with Nussbaum-type function [129].	Fuzzy T-S residual generation [14]. Fuzzy T-S sliding mode observer [90]. Adaptive extended state observer [3]. Robust adaptive fault estimation [29].	Model predictive controllers and Kalman filters are used to identify the faults [135]. Ziegler- Nichols rules are applied to adjust the PI controller parameters [130]. Robust fuzzy scheduler [112]. adaptive sliding mode observer to modify traditional PI baseline controller [32]. Fault estimation via adaptive laws within the nonlinear controller [31, 92].	
	Drivetrain	-	Set-membership approach [133]. Fuzzy T-S residual generation [14].	-	
	Generator and Converter	Fuzzy T-S multimodel and fuzzy if-then rule-based controller [128].	Set-membership approach [87]. Fuzzy T-S residual generation [14]. Fuzzy T-S sliding mode observer [90]. Robust adaptive fault estimation [29].	Ziegler- Nichols rules are applied to adjust the PI controller parameters [130]. Fault estimation via adaptive laws within the nonlinear controller [31, 92].	
	Aerodynamic characteristic change	-	Fuzzy if-then rules at farm level [25].	-	

735 The adoption of hardware redundancy is still an effective approach for FDI purposes. On the other hand, the observer
736 design techniques are significant alternatives. Kalman, H_∞ , UIO, fuzzy T-S, extended LPV and sliding mode
737 observers are the main tools, in which the wind estimation is generally needed, especially for drivetrain sensor FDI.
738 The use of both Kalman and H_∞ methods are robustly optimized to minimize the sensor noise effect on the constructed
739 residual. These methods are usually designed on a linearized model and a threshold logic is required. Moreover, the
740 fault isolation task is achieved via fault signature consideration and observer bank design. Regarding the need for
741 wind speed estimation, the UIO design represents a suitable technique to achieve robust estimation. The wind turbine
742 states and faults can be estimated simultaneously by using the extended LPV observer with adaptive observer gain.
743 However, this method is very sensitive to the model accuracy as well as its design parameters. On the other hand, the
744 fuzzy T-S observer can capture the nonlinear behavior of wind turbines. So, the modelling uncertainty effect on the
745 observer performance is reduced. However, the expert's knowledge is needed to be employed to define the proper
746 fuzzy rules. Finally, the sliding mode observer is applied to the nonlinear model, which represents a viable solution
747 for practical implementation. However, it is very sensitive to measurement noise and design parameters. The
748 missed/false fault detection rate is reduced by adopting the set-membership approach in which the threshold need is
749 removed. Nevertheless, an appropriate computational algorithm is needed. Also, the Bayesian framework can be
750 utilized to estimate the fault probability, using SCADA data. However, the sample rate of the signals from SCADA is
751 much too low for general FDI purposes. Neural networks and fuzzy systems are very appropriate for FDI design due
752 to their robustness against sensor noise, model uncertainties and wind speed variation. However, the training stage
753 requires a large amount of fault-free data.

754 For the fault tolerance feature, the VSA approach is more commonly adopted to compensate for the wind turbine
755 sensor faults. This approach has attracted most of the industrial interest due to its simple implementation. The CR
756 strategy has been considered for accommodating the wind turbine actuator faults. However, accurate fault information
757 is needed. In contrast to active FTC, the passive solutions are designed in a conservative manner, to remove the need
758 for fault detection, and meanwhile to keep the wind turbine working in faulty situations with an accepted performance
759 level, only in specific considered fault situations.

760 The mitigation of structural loads is a vital step in the control design before installation as an industrial wind turbine
761 controller. The main structural loads are blade root bending moments, tower/nacelle bending moments/acceleration
762 and drivetrain torsion moments [22]. However, most of the designed FTC schemes have been focused on the power
763 control and satisfying operational objectives [1]. For example, in [68, 137] the blade root moment sensor FDI scheme
764 is proposed, using Kalman filtering, for the accurate individual pitch control, which, in turn, reduces the blade fatigue
765 loads. Also, with proper pitch angle regulation, the aerodynamic thrust force can be controlled to reduce the applied
766 bending moment on the blades [27]. In [20, 111], the fuzzy gained scheduled PI controllers are proposed to remove
767 the actuator and sensor faults, respectively, while tower-top fore-aft and side-to-side accelerations, deflections, and
768 moments are investigated and kept at the baseline controller level, which in turn leads to an industrial acceptable
769 controller. Another promising load mitigation FTC approach is wind farm control to reduce the load on a faulty turbine
770 with satisfactory overall demanded power generation [124]. In this regard, in [25], using the proportional distribution
771 algorithm, this objective is met by generator torque correction via FIS, to avoid overloading the remaining healthy
772 turbines and intense control command. It is shown that the proposed FTC scheme has minimal impact on the structural
773 loads during fault accommodation. Finally, to lessen the drivetrain torsion, the generator speed can be band-filtered
774 prior to feeding this signal to the controller, to remove the drivetrain resonant frequency, and consequently, smooth
775 the drivetrain torsion rate [1]. Also, in [92, 129], the proposed FTC schemes are designed on the reduced drivetrain
776 torsion trajectory, to guarantee that the drivetrain torsion is kept at the baseline controller level.

777 Finally, by considering the issues above, future trends on wind turbines FDI and FTC are suggested in the following.

- 778 • Expert's knowledge can be included in the design phase, using soft computing approaches, e.g. fuzzy if-then rules,
779 neural networks or Bayesian frameworks.
- 780 • High-fidelity simulators are required for both wind turbine and wind farm systems.
- 781 • More realistic fault scenarios need to be implemented and analyzed.
- 782 • Accurate performance analysis, verification and validation tools applied to the developed FDI and FTC strategies
783 are required.
- 784 • The practical implementation of the designed schemes needs to be assessed in experimental-scale wind turbines and
785 industrial applications.
- 786 • Most of the studies have been focused on FDI, rather than FTC design. Moreover, the proposed solutions are mostly
787 developed for a given operational region of the wind turbine. Accordingly, the focus should be on FTC systems,
788 since the FDI task is a by-product. Moreover, the requirements of Industry 4.0 lead to consider adaptive and real-
789 time methodologies, working for the whole operational region of the wind turbine.

790 • Some faults are better dealt with at the wind farm control level, e.g. blade debris build-up, erosion and slowly
791 developing faults, but the literature is still scarce. So, new schemes for detection, isolation and accommodation of
792 faults at the wind farm level should be investigated.

793 • Some faults, such as the ones affecting the drivetrain, are detected only via signal-based approaches (e.g. vibration
794 or frequency analysis tools); active schemes should be analyzed for this wind turbine component.

795 **7. Conclusions**

796 In this paper, the most common model-based FDI and FTC techniques for wind turbines and wind farms were outlined
797 and reviewed, motivated by the need for more reliable wind power generation and lower operational cost. Indeed,
798 these techniques can improve the wind turbine operation not only in fault-free conditions, but also in faulty situations.
799 This review paper was prepared in a tutorial fashion to be suitably used for further studies. Firstly, different wind
800 turbine modelling tools including all possible fault situations are considered. Different FDI methods applied to wind
801 turbines were introduced and their applications to the most common fault cases were also discussed. FTC methods
802 were also outlined as a second step to achieve proper fault tolerance features. Finally, future trends were suggested to
803 drive further researchers' studies, which represent viable and effective solutions for industrial applications.

804 **Reference**

- 805 [1] Simani S. Overview of Modelling and Advanced Control Strategies for Wind Turbine Systems. *Energies*.
806 2015;8:13395-418.
- 807 [2] Council GWE. Wind Energy Statistics 2014. Global Wind Energy Council: Brussels, Belgium 10 February. 2015.
- 808 [3] Shi F, Patton R. An active fault tolerant control approach to an offshore wind turbine model. *Renew Energ*.
809 2015;75:788-98.
- 810 [4] Kabir M, Oo AM, Rabbani M. A brief review on offshore wind turbine fault detection and recent development in
811 condition monitoring based maintenance system. In *Proceedings of Australasian Universities Power Engineering*
812 *Conf (AUPEC) 2015*. p. 1-7.
- 813 [5] Knopf B, Nahmmacher P, Schmid E. The European renewable energy target for 2030 – An impact assessment of
814 the electricity sector. *Energy Policy*. 2015;85:50-60.
- 815 [6] GOTTLIEB MH. Denmark puts new record in the wind, [https://www.danskenergi.dk/nyheder/danmark-saetter-](https://www.danskenergi.dk/nyheder/danmark-saetter-ny-rekord-vind)
816 [ny-rekord-vind](https://www.danskenergi.dk/nyheder/danmark-saetter-ny-rekord-vind). *DANSK ENERGI*; 2018.
- 817 [7] Byon E, Ding Y. Season-dependent condition-based maintenance for a wind turbine using a partially observed
818 Markov decision process. *IEEE Trans Power Sys*. 2010;25:1823-34.
- 819 [8] Faulstich S, Hahn B, Tavner PJ. Wind turbine downtime and its importance for offshore deployment. *Wind Energy*.
820 2011;14:327-37.
- 821 [9] Luo N, Vidal Y, Acho L. *Wind turbine control and monitoring*: Springer; 2014.
- 822 [10] Wei X, Verhaegen M, Van den Engelen T. Sensor fault diagnosis of wind turbines for fault tolerant. *IFAC*
823 *Proceedings Volumes*. 2008;41:3222-7.
- 824 [11] Feng Z, Liang M, Zhang Y, Hou S. Fault diagnosis for wind turbine planetary gearboxes via demodulation
825 analysis based on ensemble empirical mode decomposition and energy separation. *Renew Energ*. 2012;47:112-26.
- 826 [12] McMillan D, Ault GW. Quantification of condition monitoring benefit for offshore wind turbines. *Wind*
827 *Engineering*. 2007;31:267-85.
- 828 [13] Walford CA. *Wind turbine reliability: understanding and minimizing wind turbine operation and maintenance*
829 *costs*: Department of Energy of United States; 2006.
- 830 [14] Simani S, Farsoni S, Castaldi P. Fault diagnosis of a wind turbine benchmark via identified fuzzy models. *IEEE*
831 *Trans Ind Electron*. 2015;62:3775-82.
- 832 [15] Feng Y, Tavner P, Long H. Early experiences with UK Round 1 offshore wind farms. In *Proceedings of the*
833 *Institution of Civil Engineers: energy*. 2010;163:167-81.
- 834 [16] Entezami M, Hillmansén S, Weston P, Papaalias MP. Fault detection and diagnosis within a wind turbine
835 mechanical braking system using condition monitoring. *Renew Energ*. 2012;47:175-82.
- 836 [17] Odgaard PF, Stoustrup J, Kinnaert M. Fault tolerant control of wind turbines—a benchmark model. *IFAC*
837 *Proceedings Volumes*. 2009;42:155-60.
- 838 [18] Hameed Z, Hong Y, Cho Y, Ahn S, Song C. Condition monitoring and fault detection of wind turbines and related
839 algorithms: A review. *Renew Sustain Energy Rev*. 2009;13:1-39.
- 840 [19] Leite GdNP, Araújo AM, Rosas PAC. Prognostic techniques applied to maintenance of wind turbines: a concise
841 and specific review. *Renew Sustain Energy Rev*. 2018;81:1917-25.
- 842 [20] Badihi H, Zhang Y, Hong H. Wind turbine fault diagnosis and fault-tolerant torque load control against actuator
843 faults. *IEEE Trans Cont Syst Tech*. 2015;23:1351-72.
- 844 [21] Odgaard PF, Stoustrup J, Kinnaert M. Fault-tolerant control of wind turbines: A benchmark model. *IEEE Trans*
845 *Contr Syst Tech*. 2013;21:1168-82.

- 846 [22] Badihi H, Zhang Y, Hong H. A review on application of monitoring, diagnosis, and fault-tolerant control to wind
847 turbines. In Proceedings of Conf on Control and Fault-Tolerant Systems (SysTol) 2013. p. 365-70.
- 848 [23] Hameed Z, Ahn S, Cho Y. Practical aspects of a condition monitoring system for a wind turbine with emphasis
849 on its design, system architecture, testing and installation. *Renew Energ.* 2010;35:879-94.
- 850 [24] Pourmohammad S, Fekih A. Fault-tolerant control of wind turbine systems-a review. In Proceedings IEEE
851 Green Technologies Conf 2011. p. 1-6.
- 852 [25] Badihi H, Zhang Y, Hong H. Fault-tolerant cooperative control in an offshore wind farm using model-free and
853 model-based fault detection and diagnosis approaches. *Appl Energy.* 2017;201: 284-307.
- 854 [26] Odgaard PF, Stoustrup J. A benchmark evaluation of fault tolerant wind turbine control concepts. *IEEE Trans*
855 *Cont Syst Tech.* 2015;23:1221-8.
- 856 [27] Sanchez H, Escobet T, Puig V, Odgaard PF. Fault diagnosis of an advanced wind turbine benchmark using
857 interval-based ARRs and observers. *IEEE Trans Ind Electron.* 2015;62:3783-93.
- 858 [28] Odgaard PF, Stoustrup J. An evaluation of fault tolerant wind turbine control schemes applied to a benchmark
859 model. In Proceedings of IEEE Conf on Control Applications (CCA) France2014. p. 1366-71.
- 860 [29] Simani S, Castaldi P. Active actuator fault-tolerant control of a wind turbine benchmark model. *Int J Robust*
861 *Nonlinear Cont.* 2014;24:1283-303.
- 862 [30] Burton T, Jenkins N, Sharpe D, Bossanyi E. *Wind energy handbook*: John Wiley & Sons; 2011.
- 863 [31] Habibi H, Rahimi Nohooji H, Howard I. Power maximization of variable-speed variable-pitch wind turbines
864 using passive adaptive neural fault tolerant control. *Front Mech Eng.* 2017;12:377-88.
- 865 [32] Lan J, Patton RJ, Zhu X. Fault-tolerant wind turbine pitch control using adaptive sliding mode estimation. *Renew*
866 *Energ.* 2018;116:219-31.
- 867 [33] Sloth C, Esbensen T, Stoustrup J. Robust and fault-tolerant linear parameter-varying control of wind turbines.
868 *Mechatronics.* 2011;21:645-59.
- 869 [34] Vidal Y, Tutivén C, Rodellar J, Acho L. Fault diagnosis and fault-tolerant control of wind turbines via a discrete
870 time controller with a disturbance compensator. *Energies.* 2015;8:4300-16.
- 871 [35] Tiwari R, Babu NR. Recent developments of control strategies for wind energy conversion system. *Renew Sustain*
872 *Energy Rev.* 2016;66:268-85.
- 873 [36] Lin Y, Tu L, Liu H, Li W. Fault analysis of wind turbines in China. *Renew Sustain Energy Rev.* 2016;55:482-
874 90.
- 875 [37] Bianchi FD, De Battista H, Mantz RJ. *Wind turbine control systems: principles, modelling and gain scheduling*
876 *design*: Springer Science & Business Media; 2006.
- 877 [38] Habibi H, Koma AY, Sharifian A. Power and velocity control of wind turbines by adaptive fuzzy controller
878 during full load operation. *Iran J of Fuzzy Syst.* 2016;13:35-48.
- 879 [39] Li H, Yang C, Hu Y, Liao X, Zeng Z, Zhe C. An improved reduced-order model of an electric pitch drive system
880 for wind turbine control system design and simulation. *Renewable Energy.* 2016;93:188-200.
- 881 [40] Odgaard PF, Johnson KE. Wind turbine fault detection and fault tolerant control-an enhanced benchmark
882 challenge. In Proceedings of American Control Conference (ACC)2013. p. 4447-52.
- 883 [41] Odgaard PF, Stoustrup J. Frequency based fault detection in wind turbines. *IFAC Proceedings Volumes.*
884 2014;47:5832-7.
- 885 [42] Zhang X, Zhang Q, Zhao S, Ferrari RM, Polycarpou MM, Parisini T. Fault detection and isolation of the wind
886 turbine benchmark: An estimation-based approach. In Proceedings of IFAC world congress Italy2011. p. 8295-300.
- 887 [43] Sloth C, Esbensen T, Stoustrup J. Active and passive fault-tolerant LPV control of wind turbines. In Proceedings
888 of American Control Conf (ACC) 2010. p. 4640-6.
- 889 [44] Negre PL, Puig V, Pineda I. Fault detection and isolation of a real wind turbine using LPV observers. In
890 Proceedings of 18th IFAC World Congress 2011. p. 12372-9.
- 891 [45] Simani S, Castaldi P, Tilli A. Data-Driven Approach for Wind Turbine Actuator and Sensor Fault Detection
892 and Isolation. *IFAC Proceedings Volumes.* 2011;44:8301-6.
- 893 [46] Dong J, Verhaegen M. Data driven fault detection and isolation of a wind turbine benchmark. In Proceedings of
894 IFAC World Congress 2011. p. 7086-91.
- 895 [47] Laouti N, Sheibat-Othman N, Othman S. Support vector machines for fault detection in wind turbines. In
896 Proceedings of IFAC world congress Italy2011. p. 7067-707.
- 897 [48] Simani S, Castaldi P, Tilli A. Data-driven Modelling of a Wind Turbine Benchmark for Fault Diagnosis
898 Application. *Trans Control Mechanical Syst.* 2013;1.
- 899 [49] Simani S, Castaldi P, Farsoni S. Data-Driven Fault Diagnosis of a Wind Farm Benchmark Model. *Energies.*
900 2017;10:866.

- 901 [50] Simani S, Farsoni S, Castaldi P. Wind turbine simulator fault diagnosis via fuzzy modelling and identification
902 techniques. *Sustain Energy Grid Network*. 2015;1:45-52.
- 903 [51] Chen W, Ding SX, Sari A, Naik A, Khan AQ, Yin S. Observer-based FDI schemes for wind turbine benchmark.
904 In *Proceedings of IFAC world congress Italy2011*. p. 7073-8.
- 905 [52] Salem AA, Abu-Siada A, Islam S. Condition monitoring techniques of the wind turbines gearbox and rotor. *Int J*
906 *Electric Energ*. 2014;2.
- 907 [53] Zaher A, McArthur S, Infield D, Patel Y. Online wind turbine fault detection through automated SCADA data
908 analysis. *Wind Energy*. 2009;12:574-93.
- 909 [54] Tchakoua P, Wamkeue R, Ouhrouche M, Slaoui-Hasnaoui F, Tameghe TA, Ekemb G. Wind turbine condition
910 monitoring: State-of-the-art review, new trends, and future challenges. *Energies*. 2014;7:2595-630.
- 911 [55] Odgaard PF, Stoustrup J. Gear-box fault detection using time-frequency based methods. *Annu Rev Control*.
912 2015;40:50-8.
- 913 [56] Zhang Z, Verma A, Kusiak A. Fault analysis and condition monitoring of the wind turbine gearbox. *IEEE Trans*
914 *Energy Convers*. 2012;27:526-35.
- 915 [57] Lu Y, Tang J, Luo H. Wind turbine gearbox fault detection using multiple sensors with features level data fusion.
916 *J Eng Gas Turb Power*. 2012;134:042501.
- 917 [58] Tang B, Song T, Li F, Deng L. Fault diagnosis for a wind turbine transmission system based on manifold learning
918 and Shannon wavelet support vector machine. *Renew Energ*. 2014;62:1-9.
- 919 [59] Marvuglia A, Messineo A. Monitoring of wind farms' power curves using machine learning techniques. *Appl*
920 *Energ*. 2012;98:574-83.
- 921 [60] Wenyi L, Zhenfeng W, Jiguang H, Guangfeng W. Wind turbine fault diagnosis method based on diagonal
922 spectrum and clustering binary tree SVM. *Renew Energ*. 2013;50:1-6.
- 923 [61] Liu W, Zhang W, Han J, Wang G. A new wind turbine fault diagnosis method based on the local mean
924 decomposition. *Renew Energ*. 2012;48:411-5.
- 925 [62] Odgaard PF, Stoustrup J. Fault tolerant wind farm control—A benchmark model. In *Proceedings of IEEE*
926 *International Conf on Control Applications (CCA) 2013*. p. 412-7.
- 927 [63] Qiao W, Lu D. A survey on wind turbine condition monitoring and fault diagnosis—Part I: Components and
928 subsystems. *IEEE Trans Ind Electron*. 2015;62:6536-45.
- 929 [64] Qiao W, Lu D. A survey on wind turbine condition monitoring and fault diagnosis—Part II: Signals and signal
930 processing methods. *IEEE Trans Ind Electron*. 2015;62:6546-57.
- 931 [65] Márquez FPG, Tobias AM, Pérez JMP, Papaelias M. Condition monitoring of wind turbines: Techniques and
932 methods. *Renew Energ*. 2012;46:169-78.
- 933 [66] Wilkinson M, Darnell B, van Delft T, Harman K. Comparison of methods for wind turbine condition monitoring
934 with SCADA data. *IET Renew Power Gen*. 2014;8:390-7.
- 935 [67] Odgaard PF, Damgaard C, Nielsen R. On-line estimation of wind turbine power coefficients using unknown input
936 observers. *IFAC Proceedings Volumes*. 2008;41:10646-51.
- 937 [68] Wei X, Verhaegen M, van Engelen T. Sensor fault detection and isolation for wind turbines based on subspace
938 identification and Kalman filter techniques. *Int J Adapt Control*. 2010;24:687-707.
- 939 [69] Dobrila C, Stefansen R. Fault tolerant wind turbine control: Technical University of Denmark, Kgl. Lyngby,
940 Denmark; 2007.
- 941 [70] Odgaard PF, Stoustrup J, Nielsen R, Damgaard C. Observer based detection of sensor faults in wind turbines. In
942 *Proceedings of European Wind Energy Conf 2009*. p. 4421-30.
- 943 [71] Blesa Izquierdo J, Puig Cayuela V, Romera Formiguera J, Saludes Closa J. Fault diagnosis of wind turbines using
944 a set-membership approach. *IFAC Proceedings Volumes*. 2011;44:8316-21.
- 945 [72] Odgaard PF, Stoustrup J. Results of a wind turbine fdi competition. *IFAC Proceedings Volumes*. 2012;45:102-
946 7.
- 947 [73] Ozdemir AA, Seiler P, Balas GJ. Wind turbine fault detection using counter-based residual thresholding.
948 *Proceedings of IFAC world congress 2011*. p. 8289-94.
- 949 [74] Karimi S, Gaillard A, Poure P, Saadate S. FPGA-based real-time power converter failure diagnosis for wind
950 energy conversion systems. *IEEE Trans Ind Electron*. 2008;55:4299-308.
- 951 [75] Pisu P, Ayalew B. Robust fault diagnosis for a horizontal axis wind turbine. *IFAC Proceedings Volumes*.
952 2011;44:7055-60.
- 953 [76] Jena D, Rajendran S. A review of estimation of effective wind speed based control of wind turbines. *Renew*
954 *Sustain Energy Rev*. 2015;43:1046-62.
- 955 [77] Agarwal D, Kishor N. A fuzzy inference-based fault detection scheme using adaptive thresholds for health
956 monitoring of offshore wind-farms. *IEEE Sens J*. 2014;14:3851-61.

- 957 [78] Kiasi F, Prakash J, Shah S, Lee JM. Fault detection and isolation of a benchmark wind turbine using the likelihood
958 ratio test. *IFAC Proceedings Volumes*. 2011;44:7079-85.
- 959 [79] Dey S, Pisu P, Ayalew B. A comparative study of three fault diagnosis schemes for wind turbines. *IEEE Trans*
960 *Contr Syst Tech*. 2015;23:1853-68.
- 961 [80] Odgaard PF, Stoustrup J. Unknown input observer based detection of sensor faults in a wind turbine. In
962 *Proceedings of IEEE International Conf on Control Applications* 2010. p. 310-5.
- 963 [81] Cao M, Qiu Y, Feng Y, Wang H, Li D. Study of Wind Turbine Fault Diagnosis Based on Unscented Kalman
964 Filter and SCADA Data. *Energies*. 2016;9:847.
- 965 [82] Georg S, Schulte H. Diagnosis of Actuator Parameter Faults in Wind Turbines Using a Takagi-Sugeno Sliding
966 Mode Observer. In: Korbicz J, Kowal M, editors. *Intelligent Systems in Technical and Medical Diagnostics*. Berlin,
967 Heidelberg: Springer Berlin Heidelberg; 2014. p. 29-40.
- 968 [83] Pöschke F, Georg S, Schulte H. Fault reconstruction using a Takagi-Sugeno sliding mode observer for the wind
969 turbine benchmark. In *Proceedings of International Conf on Control* 2014. p. 456-61.
- 970 [84] Chen L, Shi F, Patton R. Active FTC for hydraulic pitch system for an off-shore wind turbine. In *Proceedings of*
971 *Conf on Control and Fault-Tolerant Systems (SysTol)* 2013. p. 510-5.
- 972 [85] Odgaard PF, Stoustrup J. Model based fault tolerant observers for wind turbines. In *Proceedings of European*
973 *Wind Energy Conference and Exhibition (EWEC)* 2012. p. 1348-53.
- 974 [86] Casau P, Rosa P, Tabatabaeipour SM, Silvestre C, Stoustrup J. A set-valued approach to FDI and FTC of wind
975 turbines. *IEEE Trans Contr Syst Tech*. 2015;23:245-63.
- 976 [87] Rotondo D, Nejari F, Puig V, Blesa J. Fault tolerant control of the wind turbine benchmark using virtual
977 sensors/actuators. In *Proceedings of Fault Detection, Supervision and Safety of Technical Processes* 2012. p. 114-9.
- 978 [88] Zhang X, Zhang Q, Zhao S, Ferrari R, Polycarpou MM, Parisini T. Fault detection and isolation of the wind
979 turbine benchmark: An estimation-based approach. *IFAC Proceedings Volumes*. 2011;44:8295-300.
- 980 [89] Schulte H, Zajac M, Georg S. Takagi-Sugeno sliding mode observer design for load estimation and sensor fault
981 detection in wind turbines. In *Proceedings of IEEE International Conf on Fuzzy Systems* 2012. p. 1-8.
- 982 [90] Schulte H, Gauterin E. Fault-tolerant control of wind turbines with hydrostatic transmission using Takagi-Sugeno
983 and sliding mode techniques. *Annu Rev Control*. 2015;40:82-92.
- 984 [91] Filik ÜB, Filik T. Wind Speed Prediction Using Artificial Neural Networks Based on Multiple Local
985 Measurements in Eskisehir. *Energy Procedia*. 2017;107:264-9.
- 986 [92] Habibi H, Nohooji HR, Howard I. Optimum efficiency control of a wind turbine with unknown desired trajectory
987 and actuator faults. *J Renew Sustain Energy*. 2017;9:063305.
- 988 [93] Giebhardt J. Rotor condition monitoring for improved operational safety of offshore wind energy converters.
989 2005.
- 990 [94] Qiu Y, Feng Y, Tavner P, Richardson P, Erdos G, Chen B. Wind turbine SCADA alarm analysis for improving
991 reliability. *Wind Energy*. 2012;15:951-66.
- 992 [95] Chen B, Qiu Y, Feng Y, Tavner P, Song W. Wind turbine SCADA alarm pattern recognition. In *Proceedings of*
993 *IET Conf on Renewable Power Generation* 2011. p. 1-6.
- 994 [96] Garcia MC, Sanz-Bobi MA, del Pico J. SIMAP: Intelligent System for Predictive Maintenance: Application to
995 the health condition monitoring of a windturbine gearbox. *Comput Ind*. 2006;57:552-68.
- 996 [97] Simani S, Castaldi P, Bonfe M. Hybrid model-based fault detection of wind turbine sensors. *IFAC Proceedings*
997 *Volumes*. 2011;44:7061-6.
- 998 [98] Habibi H, Koma AY, Howard I. Power Improvement of Non-Linear Wind Turbines during Partial Load Operation
999 using Fuzzy Inference Control. *Control Eng Appl Inf*. 2017;19:31-42.
- 1000 [99] Giebhardt J. Evolutionary algorithm for optimisation of condition monitoring and fault prediction pattern
1001 classification in offshore wind turbines. In *Proceedings of European Wind Energy Conf* 2006. p. 1-9.
- 1002 [100] Tabatabaeipour SM, Odgaard PF, Bak T, Stoustrup J. Fault detection of wind turbines with uncertain parameters:
1003 a set-membership approach. *Energies*. 2012;5:2424-48.
- 1004 [101] Ribrant J, Bertling L. Survey of failures in wind power systems with focus on Swedish wind power plants during
1005 1997-2005. In *Proceedings of IEEE Power Engineering Society General Meeting* 2007. p. 1-8.
- 1006 [102] Stoican F, Raduinea C-F, Olaru S. Adaptation of set theoretic methods to the fault detection of wind turbine
1007 benchmark. In *Proceedings of IFAC World Congress* 2011. p. 8322-7.
- 1008 [103] Chen B, Tavner PJ, Feng Y, Song WW, Qiu Y. Bayesian network for wind turbine fault diagnosis. *EWEA*
1009 2012. p. 1-9.
- 1010 [104] Fernández-Cantí RM, Tornil-Sin S, Blesa J, Puig V. Nonlinear set-membership identification and fault detection
1011 using a Bayesian framework: Application to the wind turbine benchmark. In *Proceedings of 52nd Annual Conf on*
1012 *Decision and Control (CDC): IEEE*; 2013. p. 496-501.

- 1013 [105] Habibi H, Howard I, Habibi R. Bayesian Sensor Fault Detection in a Markov Jump System. *Asian J Control*.
1014 2017;19:1465–81.
- 1015 [106] Herp J, Ramezani MH, Bach-Andersen M, Pedersen NL, Nadimi ES. Bayesian state prediction of wind turbine
1016 bearing failure. *Renew Energ*. 2017.
- 1017 [107] Jihong L, Daping X, Xiyun Y. Sensor fault detection in variable speed wind turbine system using H_∞/H_∞
1018 method. In *Proceedings of 7th World Congress on Intelligent Control and Automation 2008*. p. 4265-9.
- 1019 [108] Wei X, Verhaegen M. Fault Detection of Large Scale Wind Turbine Systems: A mixed H_∞/H_∞ Index Observer
1020 Approach. In *Proceedings of the 16th Mediterranean Conf on Control and Automation 2008*. p. 1675-80.
- 1021 [109] Kamal E, Aitouche A. Robust fault tolerant control of DFIG wind energy systems with unknown inputs. *Renew*
1022 *Energ*. 2013;56:2-15.
- 1023 [110] Kamal E, Aitouche A, Ghorbani R, Bayart M. Fuzzy scheduler fault-tolerant control for wind energy conversion
1024 systems. *IEEE Trans Contr Syst Tech*. 2014;22:119-31.
- 1025 [111] Badihi H, Zhang Y, Hong H. Fuzzy gain-scheduled active fault-tolerant control of a wind turbine. *J Franklin*
1026 *Inst*. 2014;351:3677-706.
- 1027 [112] Kamal E, Aitouche A, Abbes D. Robust fuzzy scheduler fault tolerant control of wind energy systems subject
1028 to sensor and actuator faults. *Int J Elec Power*. 2014;55:402-19.
- 1029 [113] Odgaard PF, Stoustrup J, Kinnaert M. Fault Tolerant Control of Wind Turbines - Benchmark Model. In
1030 *Proceedings of Fault Detection, Supervision and Safety of Technical Processes 2009*. p. 155-60.
- 1031 [114] Rothenhagen K, Fuchs FW. Doubly fed induction generator model-based sensor fault detection and control loop
1032 reconfiguration. *IEEE Trans Ind Electron*. 2009;56:4229-38.
- 1033 [115] Rothenhagen K, Fuchs FW. Current sensor fault detection and reconfiguration for a doubly fed induction
1034 generator. In *Proceedings of Power Electronics Specialists Conf 2007*. p. 2732-8.
- 1035 [116] Rothenhagen K, Thomsen S, Fuchs FW. Voltage sensor fault detection and reconfiguration for a doubly fed
1036 induction generator. In *Proceedings of International Symposium on Diagnostics for Electric Machines, Power*
1037 *Electronics and Drives 2007*. p. 377-82.
- 1038 [117] Wu D, Liu W, Song J, Shen Y. Fault Estimation and Fault-Tolerant Control of Wind Turbines Using the SDW-
1039 LSI Algorithm. *IEEE Access*. 2016;4:7223-31.
- 1040 [118] Donders S, Verdult V, Verhaegen M. Fault detection and identification for wind turbine systems: a closed-loop
1041 analysis. Master's thesis, University of Twente. 2002.
- 1042 [119] Abuaiisha TS. General study of the control principles and dynamic fault behaviour of variable-speed wind turbine
1043 and wind farm generic models. *Renew Energ*. 2014;68:245-54.
- 1044 [120] Blesa J, Rotondo D, Puig V, Nejjari F. FDI and FTC of wind turbines using the interval observer approach and
1045 virtual actuators/sensors. *Control Eng Pract*. 2014;24:138-55.
- 1046 [121] Tabatabaeipour SM, Odgaard PF, Bak T. Fault detection of a benchmark wind turbine using interval analysis.
1047 In *Proceedings of American Control Conference (ACC) 2012*. p. 4387-92.
- 1048 [122] Kamal E, Aitouche A, Ghorbani R, Bayart M. Robust fuzzy fault-tolerant control of wind energy conversion
1049 systems subject to sensor faults. *IEEE Trans Contr Syst Tech*. 2012;3:231-41.
- 1050 [123] Johnson KE, Pao LY, Balas MJ, Fingersh LJ. Control of variable-speed wind turbines: standard and adaptive
1051 techniques for maximizing energy capture. *IEEE Control Syst Mag*. 2006;26:70-81.
- 1052 [124] Borcehrsen AB, Larsen JA, Stoustrup J. Fault detection and load distribution for the wind farm challenge. *IFAC*
1053 *Proceedings Volumes*. 2014;47:4316-21.
- 1054 [125] Badihi H, Zhang Y, Hong H. Model-free active fault-tolerant cooperative control in an offshore wind farm. In
1055 *Proceedings of 3rd Conf on Control and Fault-Tolerant Systems (SysTol) 2016*. p. 269-74.
- 1056 [126] Njiri JG, Söffker D. State-of-the-art in wind turbine control: Trends and challenges. *Renew Sustain Energy Rev*.
1057 2016;60:377-93.
- 1058 [127] Esbensen T, Sloth C. *Fault Diagnosis and Fault-Tolerant Control of Wind Turbines*: Aalborg University; 2009.
- 1059 [128] Simani S, Castaldi P. Data-Driven Design of Fuzzy Logic Fault Tolerant Control for a Wind Turbine
1060 Benchmark. *Fault Detection, Supervision and Safety of Technical Processes 2012*. p. 108-13.
- 1061 [129] Habibi H, Nohooji HR, Howard I. Adaptive PID Control of Wind Turbines for Power Regulation With Unknown
1062 Control Direction and Actuator Faults. *IEEE Access*. 2018;6:37464-79.
- 1063 [130] Simani S, Castaldi P. Adaptive fault-tolerant control design approach for a wind turbine benchmark. In
1064 *Proceedings of Fault Detection, Supervision and Safety of Technical Processes Conf 2012*. p. 319-24.
- 1065 [131] Sami M, Patton RJ. An FTC approach to wind turbine power maximisation via TS fuzzy modelling and control.
1066 *IFAC Proceedings Volumes*. 2012;45:349-54.
- 1067 [132] Odgaard PF, Stoustrup J. Fault tolerant control of wind turbines using unknown input observers. *IFAC*
1068 *Proceedings Volumes*. 2012;45:313-8.

- 1069 [133] Casau P, Rosa PAN, Tabatabaeipour SM, Silvestre C. Fault detection and isolation and fault tolerant control of
1070 wind turbines using set-valued observers. In Proceedings of 8th IFAC Symposium on Fault Detection, Supervision
1071 and Safety of Technical Processes Conf 2012. p. 120-5.
- 1072 [134] Sami M, Patton RJ. Global wind turbine FTC via TS fuzzy modelling and control. In Proceedings of 8th IFAC
1073 Symposium on Fault Detection, Supervision and Safety of Technical Processes 2012. p. 325-30.
- 1074 [135] Yang X, Maciejowski J. Fault-tolerant model predictive control of a wind turbine benchmark. In proceedings
1075 of the 8th IFAC Symposium on Fault Detection, Supervision and Safety of Technical Processes 2012. p. 337–42.
- 1076 [136] Fan L-L, Song Y-D. Neuro-adaptive model-reference fault-tolerant control with application to wind turbines.
1077 IET Control Theory A. 2012;6:475-86.
- 1078 [137] Wei X, Verhaegen M. Sensor and actuator fault diagnosis for wind turbine systems by using robust observer
1079 and filter. WiEn. 2011;14:491-516.
- 1080